

COPY RESOLUTION TEST CHART

**AD-A175 347**

(12)

**USAFSAM-TR-86-4**

**LONG-TERM BIOEFFECTS OF 435-MHz  
RADIOFREQUENCY RADIATION ON  
SELECTED BLOOD-BORNE ENDPOINTS  
IN CANNULATED RATS**

**Volume 1. Engineering Considerations**

**James C. Toler, M.S.  
Steven J. Bonasera, B.S.  
Vojin P. Popovic, Ph.D.**

**Georgia Institute of Technology  
Atlanta, Georgia 30332**

**DTIC FILE COPY**

**September 1986**

**DTIC  
ELECTE  
DEC 17 1986  
S B**

**Final Report for Period October 1982 - June 1985**

**Approved for public release; distribution is unlimited.**

**Prepared for**

**USAF SCHOOL OF AEROSPACE MEDICINE  
Aerospace Medical Division (AFSC)  
Brooks Air Force Base, TX 78235-5301**



NOTICES

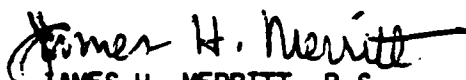
This final report was submitted by Georgia Tech Research Institute, Georgia Institute of Technology, Atlanta, Georgia, under contract F33615-83-R-0600, job order 7757-01-78, with the USAF School of Aerospace Medicine, Aerospace Medical Division, AFSC, Brooks Air Force Base, Texas. James H. Merritt (USAFSAM/RZP) was the Laboratory Project Scientist-in-Charge.

When Government drawings, specifications, or other data are used for any purpose other than in connection with a definitely Government-related procurement, the United States Government incurs no responsibility nor any obligation whatsoever. The fact that the Government may have formulated or in any way supplied the said drawings, specifications, or other data, is not to be regarded by implication, or otherwise in any manner construed, as licensing the holder, or any other person or corporation; or as conveying any rights or permission to manufacture, use, or sell any patented invention that may in any way be related thereto.

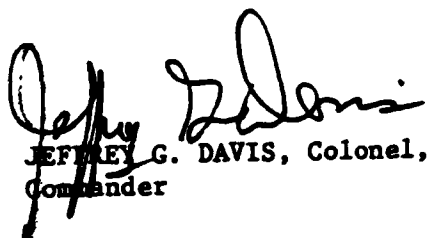
The animals involved in this study were procured, maintained, and used in accordance with the Animal Welfare Act and the "Guide for the Care and Use of Laboratory Animals" prepared by the Institute of Laboratory Animal Resources-National Research Council.

The Office of Public Affairs has reviewed this report, and it is releasable to the National Technical Information Service, where it will be available to the general public, including foreign nationals.

This report has been reviewed and is approved for publication.

  
JAMES H. MERRITT, B.S.  
Project Scientist

  
JOHN C. MITCHELL, B.S.  
Supervisor

  
JEFFREY G. DAVIS, Colonel, USAF, MC  
Commander

## REPORT DOCUMENTATION PAGE

1a. REPORT SECURITY CLASSIFICATION <b>UNCLASSIFIED</b>		1b. RESTRICTIVE MARKINGS	
2a. SECURITY CLASSIFICATION AUTHORITY		3. DISTRIBUTION / AVAILABILITY OF REPORT Approved for public release; distribution is unlimited.	
2b. DECLASSIFICATION / DOWNGRADING SCHEDULE			
3. PERFORMING ORGANIZATION REPORT NUMBER(S) GTRI Project A-3440		5. MONITORING ORGANIZATION REPORT NUMBER(S) USAFSAM-TR-86-4	
5a. NAME OF PERFORMING ORGANIZATION Georgia Tech Research Institute Georgia Institute of Technology	6b. OFFICE SYMBOL (If applicable)	7a. NAME OF MONITORING ORGANIZATION USAF School of Aerospace Medicine (RZP)	
5c. ADDRESS (City, State, and ZIP Code) 225 North Avenue, Northwest Atlanta, GA 30332		7b. ADDRESS (City, State, and ZIP Code) Aerospace Medical Division (AFSC) Brooks Air Force Base, TX 78235-5301	
3a. NAME OF FUNDING / SPONSORING ORGANIZATION	8b. OFFICE SYMBOL (If applicable)	9. PROCUREMENT INSTRUMENT IDENTIFICATION NUMBER F33615-83-R-0600	
3c. ADDRESS (City, State, and ZIP Code)		10. SOURCE OF FUNDING NUMBERS	
		PROGRAM ELEMENT NO. 62202F	PROJECT NO. 7757
		TASK NO. 01	WORK UNIT ACCESSION NO. 78
11. TITLE (Include Security Classification) Long-term Bioeffects of 435-MHz Radiofrequency Radiation on Selected Blood-borne Endpoints in Cannulated Rats. Volume 1: Engineering Considerations			
12. PERSONAL AUTHOR(S) Toler, J.C.; Bonasera, S.J.; Popovic, V.			
13a. TYPE OF REPORT Final	13b. TIME COVERED FROM Oct 1982 to Jun 1985	14. DATE OF REPORT (Year, Month, Day) 1986, September	15. PAGE COUNT 75
16. SUPPLEMENTARY NOTATION			

17. COSATI CODES			18. SUBJECT TERMS (Continue on reverse if necessary and identify by block number) Nonionizing electromagnetic radiation; radiofrequency radiation; microwave long-term bioeffects.
FIELD 06	GROUP 18	SUB-GROUP	

19. ABSTRACT (Continue on reverse if necessary and identify by block number)

This report details the engineering consideration of a program designed to monitor selected blood-borne hormones in male Sprague-Dawley rats exposed to 435-MHz continuous-wave radiofrequency radiation. The experimental group consisted of 100 rats housed in Plexiglas cages arrayed on the tiers of a stacked, parallel-plate circular waveguide. The power density along the circumference of the waveguide was 1.0 mW/cm<sup>2</sup>. The control group consisted of 100 rats housed in an identical, but unenergized, colocated facility. This volume details waveguide and antenna development, cage development, and equipment and facility descriptions.

20. DISTRIBUTION / AVAILABILITY OF ABSTRACT <input checked="" type="checkbox"/> UNCLASSIFIED/UNLIMITED <input type="checkbox"/> SAME AS RPT. <input type="checkbox"/> DTIC USERS		21. ABSTRACT SECURITY CLASSIFICATION UNCLASSIFIED	
22a. NAME OF RESPONSIBLE INDIVIDUAL James H. Merritt		22b. TELEPHONE (Include Area Code) (512) 536-3583	22c. OFFICE SYMBOL USAFSAM/RZP

86 12 17 023

## TABLE OF CONTENTS

		Page
I.	INTRODUCTION.....	1
II.	WAVEGUIDE AND ANTENNA CONSIDERATIONS.....	3
	Possible Radiation Facility Concepts.....	3
	Circular Waveguide Concept.....	3
	Free-Space Radiation Concept.....	5
	Compact Range Radiation Concept.....	6
	Circular, Parallel-Plate Radiation Concept.....	8
	Radiation Facility Recommendation.....	10
	Prototype Radiation Facility Evaluation.....	10
	Antenna Development.....	10
	Circular Parallel-Plate Waveguide.....	14
III.	CONSTRUCTION OF CIRCULAR PARALLEL-PLATE WAVEGUIDE.....	16
	Circular, Parallel Plates.....	16
	Slotted-Cylinder Antenna.....	20
IV.	TRANSMITTER SYSTEM.....	23
	Transmitter Subassemblies.....	23
	High Voltage Power Supply Subassemblies for #1 and #2 Power Amplifiers.....	26
	High Voltage Power Supply Subassembly for #1 and #2 Driver Amplifiers.....	26
	Oscillator, Preamp, and Modulator Subassembly.....	26
	System Control Subassembly.....	26
	#1 and #2 Driver Amplifier Subassembly.....	27
	#1 and #2 Power Amplifier Subassembly.....	28
	Circulator Load Subassembly.....	28
V.	ANALYSIS OF ANTENNA, DISTRIBUTION, AND PARALLEL PLATE SYSTEMS.....	30
VI.	CAGE CONSIDERATIONS.....	38
	Cage Design Considerations.....	38
	Cage Separation Consideration.....	53
VII.	CAGE WASHER SYSTEM.....	57
VIII.	DATA ACQUISITION SYSTEM.....	59
IX.	ELECTRONIC BALANCE SYSTEM.....	61

	<u>Page</u>
X. OVERALL FACILITY DESCRIPTION.....	63
XI. REFERENCES.....	67

**LIST OF FIGURES**

<u>Fig. No.</u>		<u>Page</u>
1.	Formation of a slotted-cylinder antenna.....	12
2.	Typical radiation pattern at 440 MHz obtained with prototype circular, parallel-plate waveguide and slotted-cylinder antenna.....	15
3.	Details of plate construction showing the eight petals.	17
4.	Pedestal used to support circular, parallel-plate waveguides.....	19
5.	Technique used to assemble slotted-cylinder antenna....	21
6.	Technique used to mount cables to slotted-cylinder antenna.....	22
7.	Photograph of MICON Model R9DAT Transmitter.....	24
8.	Block diagram of MICON Model R9DAT Transmitter.....	25
9.	Diagram of impedance transforming balun.....	34
10.	Styrofoam cage design for housing rats during continuous electromagnetic radiation exposure.....	43
11.	Plexiglas cage for housing rats during continuous radiation exposure.....	45
12.	Model used to evaluate effect of exposure field on watering provisions.....	47
13.	Comparison of body weight of rats housed in Plexiglas cages to rats housed in standard metal cages.....	50
14.	Comparison of body temperature of rats housed in Plexiglas cages to rats housed in standard metal cages.	51
15.	Final cage design showing changed water bottle and food hopper positions.....	53
16.	Cage Washer.....	58

<u>Fig. No.</u>		<u>Page</u>
17.	Electronic balance/data acquisition system.....	62
18.	Overall layout of the RFR facility.....	64

**LIST OF TABLES**

<u>Table No.</u>		
1.	Overall Performance Specifications for MICON Model R9DAT Transmitter.....	29
2.	Results of Measurements to Determine Effects of Exposure Field on Water Provisions.....	48

**S** DTIC ELECTE **D**  
 DEC 17 1986  
**B**

Accession For	
NTIS GRA&I	<input checked="" type="checkbox"/>
DTIC TAB	<input type="checkbox"/>
Unannounced	<input type="checkbox"/>
Justification	
By	
Distribution	
Availability Codes	
Dist	Special
A-1	





**LONG-TERM BIOEFFECTS OF 435-MHZ RADIOFREQUENCY RADIATION  
ON SELECTED BLOOD-BORNE ENDPOINTS IN CANNULATED RATS.  
VOLUME 1: ENGINEERING CONSIDERATIONS**

**I. INTRODUCTION**

The past century can be viewed in terms of its unprecedented emphasis on applying physical factors and advanced technical developments to solve society's problems. The emphasis is evident in expressions such as "the space age" and "the atomic age" that have been coined and now find common usage. Each of the areas identified in these expressions extensively uses electromagnetic waves, although the waves may occur at vastly different frequencies. The emphasis on electromagnetic wave applications in technical and societal areas can be understood in terms of man's continuing search for new methods of beneficially using electromagnetic energy. However, as electromagnetic waves continue to find more and more applications, it is not unreasonable to expect that concomitant side effects which are less than thoroughly understood might result. Such side effects have, in fact, been observed, and an expanding concern has evolved over the last two decades as it has been noted that these side effects extend to biological as well as electrical systems. The observation has spawned a considerable amount of research in complex areas of the engineering and biological disciplines. Results of this research have clarified significantly the mechanisms by which electromagnetic waves interact with biological systems and the thermal effects that inevitably result from exposure to high-level waves. Much less understood at this point are biological effects--either thermal or athermal--that might result from exposure to low-level waves, especially where the low-level exposure exists over a long time period.

This report details the engineering considerations of a program designed to monitor selected blood-borne hormones in male Sprague-Dawley rats exposed to 435-MHz continuous-wave (CW) radiofrequency (RF) radiation. The experimental group consisted of 100 rats housed in Plexiglas cages arrayed on the tiers of a stacked, parallel-plate circular waveguide. The power density along the circumference of the waveguide was  $1.0 \text{ mW/cm}^2$ . The control group consisted of

100 rats housed in an identical, but unenergized, collocated facility. The following sections detail waveguide and antenna development, cage development, and equipment and facility descriptions.

## II. WAVEGUIDE AND ANTENNA CONSIDERATIONS

Two research programs preceded the effort to actually construct a facility for long-term, low-level radiofrequency radiation (RFR) exposure of large rodent populations. In the first of these two programs, several commonly used and new RFR facility concepts were theoretically analyzed to determine their adequacy for long-term bioeffects studies in the 420-to-450 MHz frequency range. One of these concepts--the circular, parallel-plate concept--was identified as providing a technically adequate and cost-effective approach to the RFR facility. A prototype of this concept was constructed and extensively evaluated during the second research program. The results from these two programs are summarized as reference information for the following discussion of the final RFR facility construction and evaluation.

### Possible Radiation Facility Concepts

The initial program (1) analyzed both new and commonly used RFR facility concepts to determine their adequacy for long-term bioeffects studies involving large rodent populations exposed to 420-to-450 MHz fields. These concepts included:

- the circular waveguide radiation concept,
- the free-space radiation concept,
- the compact range radiation concept, and
- the circular, parallel-plate radiation concept.

Primary technical considerations during the concept analyses were exposure field configurations, ease of animal access, dosimetry, and nonperturbing provisions for water and food delivery. Also, nontechnical matters such as construction/maintenance costs and floor space requirements were also considered. The major results of these analyses for each RFR concept are summarized.

#### Circular Waveguide Concept

Individual waveguides house the experimental animals during radiation exposure. Attractive features include:

- the field incident on a given animal is not influenced by

scattering from other animals and their cages,

- the waveguides can be located in close proximity to one another, thereby minimizing floor space requirements without compromising easy observation of the animals, and
- continuous monitoring of input and output power provides a theoretically straightforward procedure for dosimetry determinations.

In a typical application (2), the  $TE_{11}$  mode will propagate in waveguides excited by 2 radial probes positioned  $90^\circ$  apart and driven with a  $90^\circ$  phase difference. The specific absorption rate (SAR) of individual animals is determined by measuring the difference between input and output powers, and dividing the difference by the mass of the animal (3).

In the analysis of this concept, electromagnetic fields in the circular waveguide were derived and the results were used to develop a design for a 450-MHz system capable of providing a  $1.0 \text{ mW/cm}^2$  incident power density. The analysis began by deriving the  $TE_{11}$  mode field configurations in the waveguide for the case of single-probe excitation, and then progressing to the case of two-probe excitation. The dominant  $TE_{11}$  mode propagates under the conditions

$$0.293 \frac{v}{f} < a < 0.383 \frac{v}{f} \quad (1)$$

where  $v$  is the speed of light in the dielectric filling the waveguide,  $f$  is the frequency, and  $a$  is the inside radius of the waveguide. Analysis of the single-probe excitation indicated that the relative power distribution across the circular waveguide had both  $\phi$ - and  $r$ -dependence ( $\phi$  is the angular position and  $r$  is the waveguide radius). For the  $\phi$ -dependence, the greatest change in power distribution across the waveguide occurred at  $\phi = 0$  and  $\phi = \pi$ . For the  $r$ -dependence, the power distribution was greatest at the waveguide center, and decreased to a minimum at the waveguide wall. For a radius of less than  $0.49a$  in the cylinder, the power density was everywhere greater than 50% of the maximum. For the case of a two-probe excitation, the power density retained the same  $r$ -dependence but lost all  $\phi$ -dependence. Also, for this excitation, energy near the waveguide center propagated with circular polarization. The region where propagation was nearly circular comprised about 6% of the total cross-sectional area of the waveguide.

Based on the single-probe and dual-probe analyses, we concluded that the waveguide diameter to propagate 450 MHz would have to be between 42.5 and 50.8 cm (17 and 20 in.). Impedance matching between the probes and the chamber dictated a waveguide length of about 1.8 m (6 ft). Input power to provide a 1 mW/cm<sup>2</sup> power density would be about 2.0 W/waveguide. A materials cost of \$224,000 was estimated for construction of 200 waveguides, assuming aluminum and expanded aluminum mesh to be the primary construction materials.

#### Free-Space Radiation Concept

A suitable antenna illuminates an array of animal cages positioned on a contour shaped in a manner to assure that all cages receive the same incident power density. The equal-power-density contour is achieved by positioning off-axis cages closer to the source antenna. In previous applications (4), the concept has been used to expose relatively small numbers of experimental animals in a configuration where the radiation axis was horizontal. For an application involving 100 radiated and 100 control rats, a vertical radiation axis was preferred to minimize cage support difficulties and ease cage cleaning and observation tasks.

An open-ended circular waveguide with a 180° corrugated flange was selected from several candidate antennas for the illuminator. The antenna has equal E- and H-plane beamwidths of about 65°, and both measured and theoretical patterns are readily available for analysis. Using a typical radiation pattern, dimensions for an equal-power-density contour were calculated as a function of the off-axis radiation angle. Cages positioned on this contour formed circular rings, and the horizontal distance from the radiation axis to each ring was the circle radius. Both the radius and the vertical dimension between 1 ring of cages and the next were functions of the cage-to-cage separation that had to be provided to maintain intercage scattering within tolerable limits. For a radiation system with the on-axis cage 4.57 m (15 ft) from the source antenna and an intercage spacing of 45.7 cm (18 in.), it was shown that 125 cages could be accommodated in 7 rings of cages.

Calculations of transmitter output power necessary to provide a 1.0 mW/cm<sup>2</sup> exposure environment for this radiation concept were made assuming a 9 dB gain for the open-ended waveguide antenna with circular polarization. The polarization was necessary because the rat cages were positioned tangent to

the equal-power-density contour; therefore, if the source antenna were linearly polarized, the incident electric field would be parallel to the long dimension of only a part of the animals. For the circularly polarized antenna, a transmitter output power of 600 W would provide the 1 mW/cm<sup>2</sup> exposure environment. The materials cost for 2 identical contours (1 for radiated animals and 1 for controls) and antennas was estimated to be \$174,000.

#### Compact Range Radiation Concept

The exposure environment is generated over a predictable volume near the aperture of a full or cut paraboloidal reflector (5,6). The concept can produce an exposure environment with a planar phase front very near the aperture (7). The exposure beam is collimated to minimize any reflections. This arrangement permits the generation of a plane-wave exposure environment in a reasonably sized indoor facility. The collimation through the plane-wave volume makes the exposure environment range independent, and therefore essentially constant as a function of distance from the aperture. The exact location of the animals within the exposure volume is of minimal concern. Although the plane wave is not completely uniform in amplitude (because of illumination taper and space attenuation), proper selection of the feed antenna and reflector will generate an environment that is about uniform over an appreciable area. Feed antenna design will determine the exposure environment polarization. Either linear or circular polarizations are easily provided.

The reflector necessary for radiating 100 rats in this compact range system would be shaped similar to a paraboloid of revolution. A paraboloid of revolution can be defined as the locus of points equidistant between a given point (called the focal point) and an imaginary plane erected perpendicular to the axis of the paraboloid. Rays reflected by the paraboloid will have points of constant phase on the imaginary plane. Also, a point source of electromagnetic energy placed at the focal point of a paraboloidal reflector will provide a plane-wave exposure environment over an area close to the reflector. The environment will propagate parallel to the reflector axis. At a distance corresponding to several reflector radii, the beam becomes a good approximation of a plane wave.

Besides a planar phase front, the exposure environment must also provide a uniform amplitude over the area occupied by the experimental animals. However, as the electromagnetic energy propagates from the focal point to the reflector surface, it diverges as a spherical wave. In the spherical wave, some energy will travel a greater distance between the focal point and reflector than other energy, and this will result in a nonuniform amplitude distribution. To correct this, the amplitude pattern of the feed antenna at the focal point must be shaped to compensate for the different distances traveled by the energy in reaching the reflector surface.

In most applications, the feed antenna is not shaped to provide amplitude uniformity over the exposure area. Instead, experimentation has shown that an amplitude nonuniformity of about 1.0 dB is generally acceptable and will exist over an exposure area equal to about one-half of the reflector aperture. Therefore, a reflector with an aperture of 3.6 m x 3.6 m (12 ft x 12 ft) will provide an exposure area about 1.8 m (6 ft) in diameter and an amplitude uniformity of 1.0 dB or better.

It is difficult to satisfactorily illuminate the entire surface of a circular paraboloidal reflector. If this illumination were attempted, the energy propagating for some portions of the reflector would be incident on the feed antenna support structure. Diffraction of this energy by the structure introduces interference patterns that destroy the uniform and planar character of the exposure environment. For these reasons, only the upper portion of the circular reflector is normally used in compact range designs. Effects due to the lower portion of the paraboloidal reflector are ignored.

During the feasibility analysis, the primary concerns were the quality of the exposure environment that could be generated over an area capable of accommodating 100 rats with an intercage spacing adequate for eliminating unacceptable scattering, and the physical dimensions of the resulting compact range. The concern with exposure environment quality involved factors such as feed antenna design, smoothness tolerances on the reflector surface, and dosimetry. Similarly, concern with physical dimensions involved factors such as floor space requirements, ceiling height requirements, animal accessibility, and construction costs. The point-of-departure in analyzing the compact range radiation concept was the fact that the usable exposure area will be about one half of the reflector aperture. Graphical techniques were

used to determine the reflector size necessary to accommodate 100 individually housed rats with an intercage spacing of 45.7 cm (18 in.). These techniques revealed that a reflector aperture about 10 m x 10 m (33 ft x 33 ft) would be necessary. These dimensions obviously presented significant difficulties in housing and constructing the reflector as well as problems in accessing the animals during the radiation study. Numerous technical approaches for reducing the reflector dimensions were considered, but all introduced unacceptable compromises in either amplitude or phase characteristics of the exposure environment.

Because of its excessive size, the compact range was not considered feasible as a radiation concept. However, material costs for constructing the reflector, and transmitter output power requirements were estimated. These estimates were \$523,000 and 2250 W, respectively.

#### Circular, Parallel-Plate Radiation Concept

There was no indication in the open literature that circular, parallel-plate waveguides had been considered as a radiation concept for bioeffects studies involving large rodent populations. However, these waveguides can be fed at their center in such a way that energy travels radially outward to a circular array of animal cages. With the feed antenna and parallel plates designed for circular symmetry, the exposure field will also exhibit circular symmetry, and all caged animals will be exposed to the same field.

The field configuration in circular, parallel-plate waveguides is a function of the spacing between the plates. For example, if the plate spacing is less than one-half wavelength, only the dominant TEM mode propagates. In this mode, the electric field is normal to the plates and the resulting polarization is vertical. If spacing between the plates is greater than one-half wavelength, both the TE and TM modes propagate. For the TE mode, the electric field is parallel to the plates and the resulting polarization is horizontal. If plate spacing is maintained greater than one-half wavelength but less than one wavelength, only the lowest-order TE mode propagates. In general, the TM modes that propagate in parallel-plate waveguides with spacing greater than one-half wavelength are of no interest in bioeffects studies because of the nonmagnetic nature of biological materials. Also, these modes are vertically polarized and would couple minimally to experimental animals.



The feasibility analysis for the circular, parallel-plate radiation concept began with the assumption that  $n$  cages were to be arrayed around the plate periphery. With a plate diameter of  $D$  and intercage separation of  $h$ , the equation

$$D = \frac{nh}{\pi} \quad (2)$$

was used to calculate a family of plate diameters as functions of cage spacing and number. These calculations showed that, for 100 cages with an intercage separation of 45.7 cm (18 in.), a plate diameter of 14.6 m (48 ft) would be required. Obviously, this plate diameter was not feasible; however, the radiation concept is maintained if several sets of waveguides are stacked on top of one another in a tier arrangement. By stacking plates, smaller plate diameters can be used to expose 100 animals while maintaining the 45.7 cm (18 in.) cage separation. In fact, 4 sets of stacked plates with 3.6 m (12 ft) diameters would be adequate for exposing 100 animals whose intercage separation was 45.7 cm (18 in.).

As noted earlier, spacing between the plates had to be maintained greater than one-half wavelength but less than one wavelength for propagation of the lowest-order TE mode. With a frequency of 435 MHz (midway in the 420-to-450-MHz frequency range of interest), this criterion translated to

$$13.57 < S < 27.14, \quad (3)$$

where  $S$  is the spacing between plates in inches. A plate spacing of 45.7 cm (18 in.) was conveniently chosen. An area with a 6.1 m x 6.1 m (20 ft x 20 ft) floor space and 3 m (10 ft) ceiling height will adequately house a facility containing 4 sets of 3.6 m (12 ft) diameter plates separated by 45.7 cm (18 in.). The floor space permits appropriate microwave absorbing material 45.7 cm (18-in.-thick material offers -30 dB reflectivity at 500 MHz) to line the facility walls, and sufficient space around the plates to access the animals.

The remaining considerations were calculations of power density variation across the height and width of cages used to house the rats, antenna types suitable for feeding the waveguide structures, transmitter output power

requirements, and overall facility cost. Calculations of power density variation noted that the TE mode exposure environment provided a cosine-squared distribution between the plates. These calculations showed that variations in both vertical and horizontal power density across an animal cage were less than 0.5 dB, and were therefore acceptable. A small loop antenna positioned at the center of each set of plates was recommended as the feed antenna. Transmitter output power calculations revealed that about 105 W would provide a  $1.0 \text{ mW/cm}^2$  exposure environment between the plates. The estimated cost of materials for construction of a circular, parallel-plate radiation facility was \$64,000.

#### Radiation Facility Recommendation

At the conclusion of the initial program, we recommended that a prototype circular, parallel-plate waveguide be constructed and evaluated. The evaluation would require that a small loop antenna also be designed and constructed, and that 25 rat cages be constructed so the waveguide could be fully loaded during its evaluation. The power source for the facility could be provided by available signal generators and amplifiers; however, the development of a transmitter design was recommended. The evaluation would be primarily concerned with determining the adequacy of the loop-feed antenna and probing the uniformity of the exposure field in the azimuth plane. Also, the 45.7-cm (18 in.) intercage separation distance would be investigated by scattering measurements to determine its adequacy.

#### **Prototype Radiation Facility Evaluation**

During the first follow-on program (8), recommendations made at the conclusion of the initial program were implemented essentially verbatim. Therefore, design considerations for a feed antenna were developed, a prototype, single set of circular, parallel plates was constructed and evaluated, 25 rat cages were constructed, and a transmitter design was developed. These efforts are summarized in the following paragraphs.

#### Antenna Development

During the initial program, Toler et al. (1) recommended that small loop

antennas be used to feed the parallel-plate waveguide. Therefore, the program's initial efforts were directed toward small loop design considerations (9). These efforts resulted in semirigid coaxial cable with a 0.212-cm (0.085 in.) diameter being used to construct a loop with a diameter of 3.12 cm (1.25 in.). Concurrently, a pair of circular plates with a 0.9-m (3 ft) diameter was constructed using aluminum-backed hardboard. Construction of these plates allowed for changes in the plate separation distance. Using frequency scaling and a network analyzer, this parallel-plate waveguide and loop antenna configuration was evaluated to determine resonant frequency and antenna efficiency as a function of plate spacing. The resonance observed was extremely sharp with a center frequency of 1.256 GHz. The antenna efficiency was about 5%.

Since the circular plate/loop antenna configuration was yielding sharp resonances and extremely low loop efficiencies, efforts to identify a more suitable antenna were begun. These efforts resulted in slotted cylinders being considered as the feed antenna for the parallel plates. As the name implies, these antennas consist of hollow metal cylinders with rectangular slots cut along their axial dimensions (10,11). The antennas have been most widely used in applications where horizontal polarization with an essentially constant amplitude horizontal pattern is required. Consequently, slotted-cylinder antennas have been used as radiators for frequency-modulated (FM) radio and ultra-high-frequency (UHF) television broadcasting. Performance of slotted-cylinder antennas can be understood by considering the slot to be fed by a coaxial cable routed along the inside of the cylinder. If the impedance around the cylinder circumference is sufficiently low, current will flow in horizontal loops around the cylinder. Under these conditions, a vertical slotted cylinder will radiate a horizontally polarized field (Fig. 1). The amplitude of this field in the horizontal plane is dependent on the cylinder diameter. In general, the radiated field amplitude tends to be greater on the cylinder side where the slot is located. However, if the cylinder diameter is sufficiently small (about one factor of magnitude) compared to the wavelength, then the radiated field in the horizontal plane becomes essentially uniform. If the cylinder diameter is increased to the point of becoming a significant part of a wavelength, the field in the region of the shadow cast by the cylinder becomes small. Generally, as the cylinder diameter becomes large, the horizontal field approximates a cardioid (12).

Slot width influences the capacitive loading of the antenna in much the

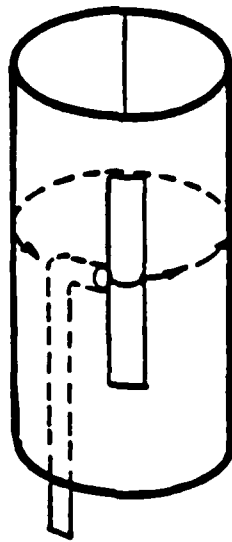
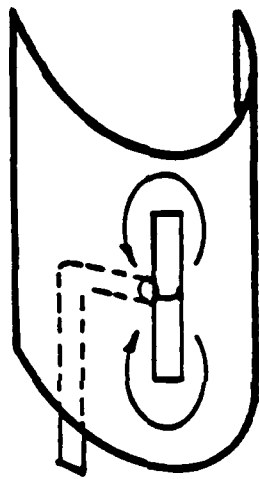
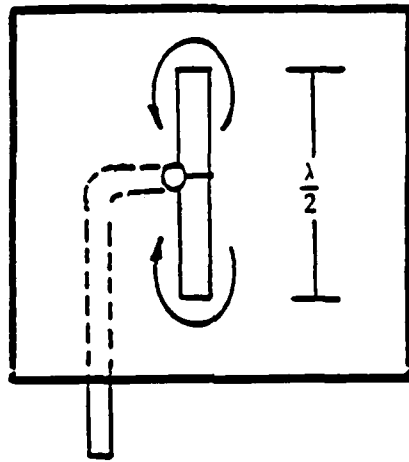


Figure 1. Formation of a slotted cylinder antenna.

same way as cylinder circumference influences inductive loading. When slot width is small relative to wavelength, the horizontal pattern is independent of the axial distribution of the field along the slot. For slotted cylinders, the effect of greater slot width is to increase the length of the slot required for resonance for a given cylinder diameter. Resonant length tends to become quite long as cylinder diameter becomes small, but decreases as the cylinder diameter increases. Thus, the interactive relationship between slot width, slot length, and cylinder diameter is evident.

A major concern in considering the slotted cylinder as a feed antenna for the circular, parallel-plate waveguide was input impedance. The impedance can be varied over a rather large range by changing the effective capacitance. For center-fed cylinders with diameters small relative to wavelength, the impedance at the first resonant point is rather high, with a range of 300 to 1000 ohms. This impedance indicates that the feed should be a parallel-wire transmission line, perhaps with an inline balun. If cylinder diameter is appreciably increased, a second resonant point occurs, and it has an impedance of about 40 ohms. This impedance indicates that the feed should be a coaxial cable. These impedance values can be varied somewhat by feeding the antenna off center.

The bandwidth and radiation pattern were a matter of interest in considering the slotted cylinder as the feed antenna for the circular, parallel-plate waveguide. Published information on bandwidth was almost nonexistent; however, reference was made in one instance (11) to measurements that indicated bandwidths at the first resonance of between 4% and 8%. These measurements were made at frequencies where the standing wave ratio on the feed line was 2:1. Published information on radiation patterns was somewhat more available, but it involved theoretically derived, rather than experimentally measured data. Theoretically derived patterns (12,13) showed essentially uniform amplitudes in the horizontal plane.

After extensively analyzing the design and performance features of slotted-cylinder antennas, a design effort was undertaken to tailor such an antenna for use with a circular, parallel-plate waveguide. The primary parameters to be defined, and their final design values, were:

- D — diameter of the cylinder — 10 cm (4 in.),
- T — thickness of the cylinder wall — 0.312 cm (0.125 in.),

- L -- length of the slot -- 35.6 cm (14 in.), and
- W -- width of the slot -- 0.312 cm (0.125 in.).

A commercially available aluminum cylinder with a 10-cm (4 in.) diameter and a 0.312-cm (0.125 in.) wall thickness was obtained, and the desired slot was cut along its axial dimension. After construction of the circular, parallel-plate waveguide, this antenna was installed and performance evaluations were conducted.

#### Circular Parallel-Plate Waveguide

A prototype set of circular, parallel plates with 3.6 m (12 ft) dia and 45.7 cm (18 in.) separation spacing was constructed and evaluated. However, the size of the largest available anechoic chamber would accommodate plates with a maximum diameter of 2.44 m (8 ft). Therefore, 2.44 m (8 ft) dia plates were constructed using aluminum-backed Styrofoam sheets and wooden supports. The Styrofoam sheets were 1.22 m x 2.44 m x 2.54 cm thick (4 ft x 8 ft x 1 in. thick), joined together using conductive tape, then trimmed to a 2.44 m (8 ft) diameter circle. Wooden supports were glued to the Styrofoam side of the sheet to provide rigidity. These supports were hinged in a way that allowed each plate to be folded in half in order to enter the anechoic chamber door. Styrofoam blocks with a 0.3048 m (1 ft) square base and a 45.7-cm (18 in.) height were used as spacers between the 2 plates. A 10-cm (4 in.) diameter hole was provided in the center of each plate to permit installation and removal of feed antennas. In the anechoic chamber, these plates were mounted on an antenna positioner that was attached to the chamber floor below the absorbing material.

The resulting circular, parallel plates provided a lightweight and inexpensive waveguide adequate for evaluating the facility concept. With the slotted-cylinder antenna in position, coupling, voltage standing-wave ratio (VSWR), radiation pattern, and scattering evaluations were conducted. About 150 pattern recordings were made to characterize the prototype waveguide's performance under a variety of parallel plate and slotted antenna conditions. Typically, a slot 36.83-cm (14.5 in.) long and 0.1587-cm (0.0625 in.) wide provided resonance at 440 MHz and a peak-to-peak horizontal field amplitude uniformity of 2 dB or less in the azimuth plane. The cross-polarized component of the field was 15 dB or more below the horizontal component. A typical radiation pattern is shown in Figure 2.

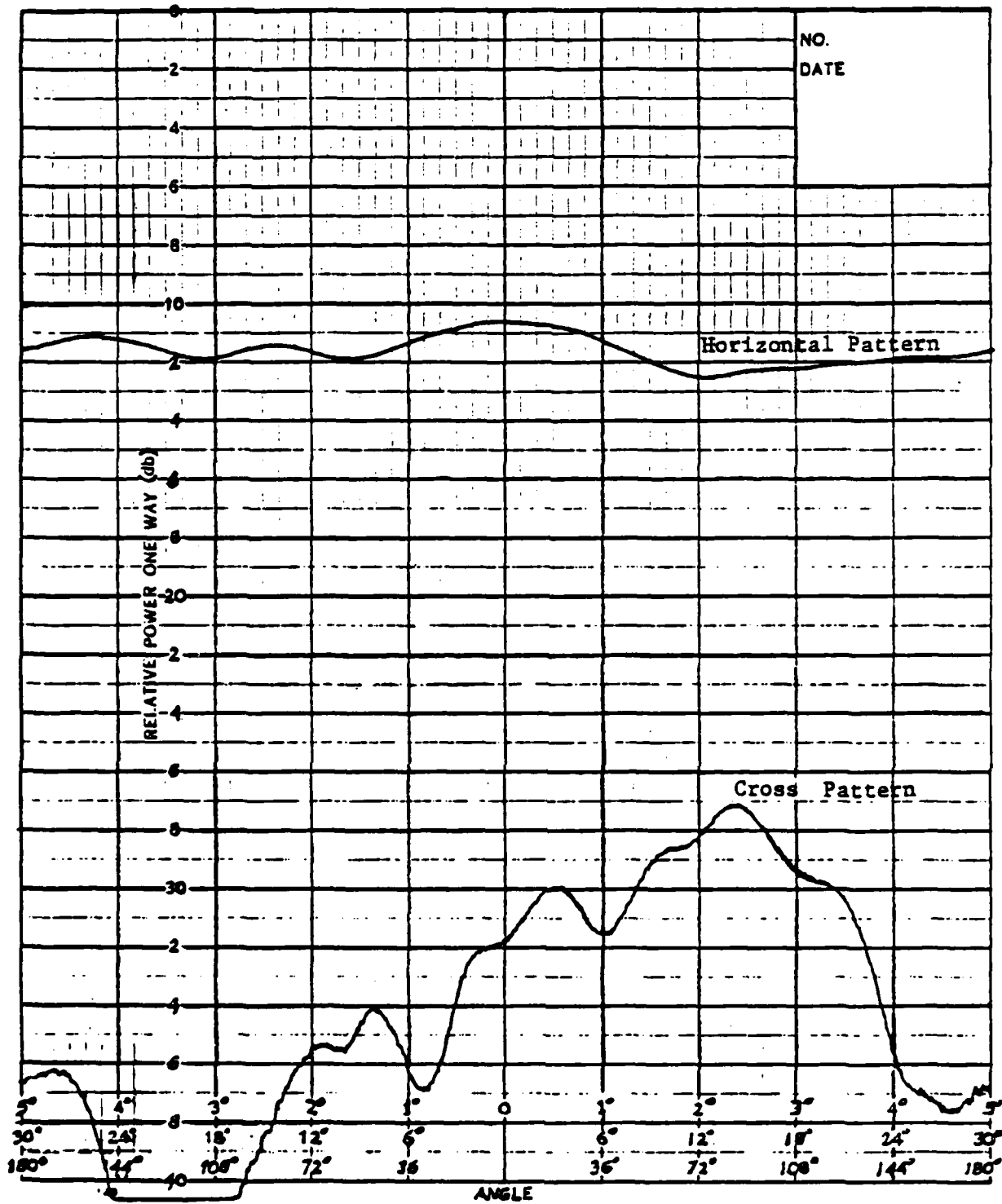


Figure 2. Typical radiation pattern at 440 MHz obtained with prototype circular, parallel-plate waveguide and slotted-cylinder antenna.

### III. CONSTRUCTION OF CIRCULAR PARALLEL-PLATE WAVEGUIDE

As pointed out earlier, a single-tier prototype model of the circular, parallel-plate waveguide and its slotted-cylinder feed antenna were constructed and evaluated. Since the evaluation results clearly indicated the feasibility of the radiation concept, design and construction began on the full-scale facility consisting of 2 identical four-tier assemblies of circular, parallel plates with slotted-cylinder feed antennas.

#### Circular, Parallel Plates

The 2 four-tier assemblies of circular, parallel plates (1 for exposure and 1 for control animals) were constructed using 10 circular aluminum plates with 3.6-m (12 ft) diameters. Five circular plates made up the exposure waveguide while the remaining 5 circular plates made up the control waveguide. The design of these plates had to allow for the possibility of moving the entire facility to another location at some future date. Therefore, each plate was constructed of 8 petals, each with a 1.8-m (6 ft) outer radius and a width dictated by a  $45^\circ$  central angle. Lap joints 2.54-cm (1 in.) wide were milled on the 2 radial edges of each petal to provide mating surfaces necessary for joining 8 adjacent petals into 1 complete plate. Type 6061-T6 aluminum sheet metal with a 0.4687-cm (0.1875 in.) thickness was selected for the petals since it was relatively lightweight, easily machined, and sufficiently thick to provide the necessary structural strength and mating surfaces for lap joints. A total of 85 (5 spares) of these petals were cut from 3.6 m x 1.8 m (12 ft x 6 ft) of Type 6061-T6 aluminum. The fabrication involved sizing each petal to a  $45^\circ$  central angle, and then cutting a 1.8-m (6 ft) diameter outer radius and a 5-cm (2 in.) diameter inner radius on each petal. The inner radius provided a 10-cm (4 in.) hole in the center when 8 petals were joined together to form a plate. The hole was used for installation of the slotted-cylinder antenna. After petals were cut to the proper size, lap joints were milled along the radial edges of each petal. A drawing of the 8 petals assembled into a plate is shown in Figure 3.



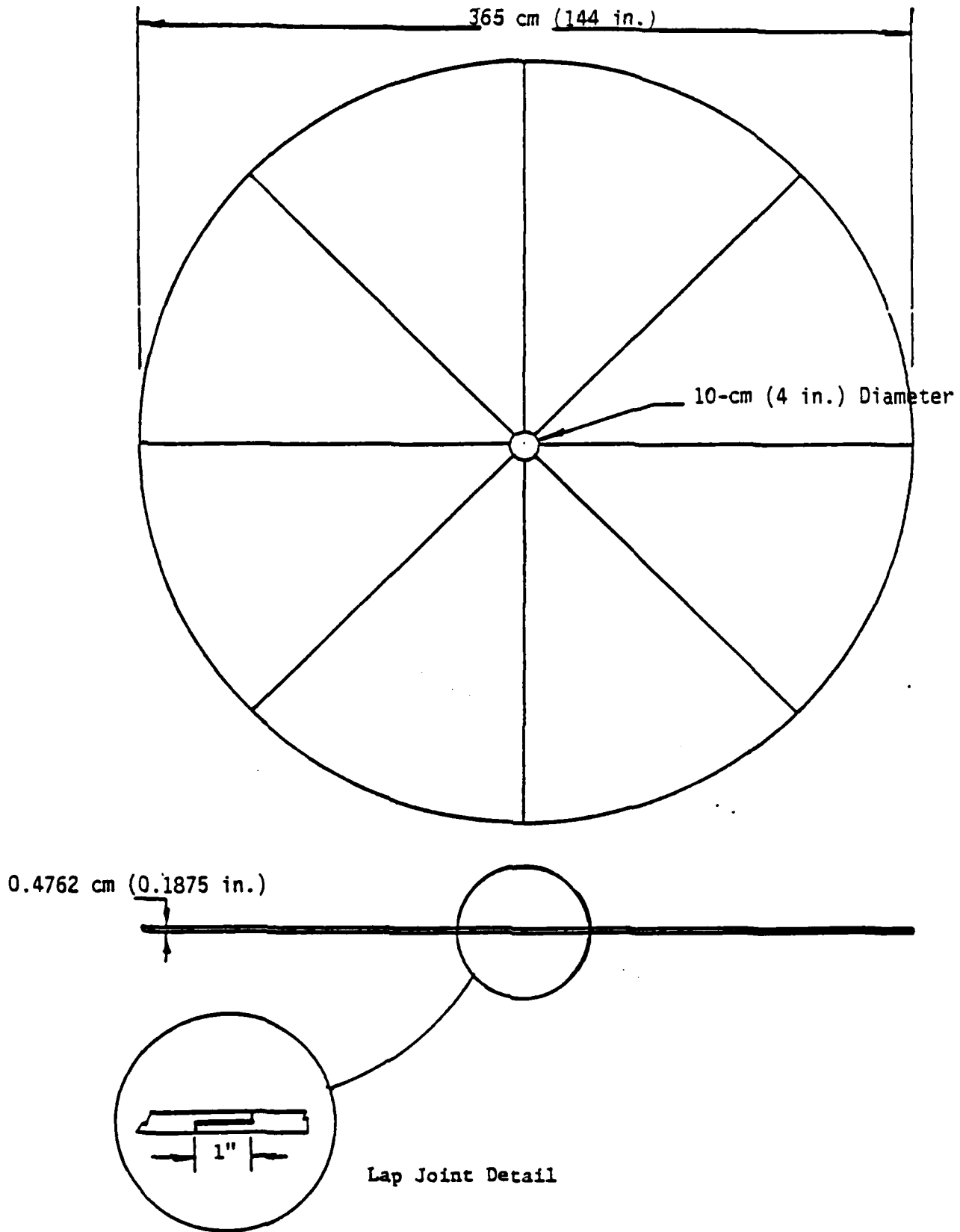


Figure 3. Details of plate construction showing the 8 petals.

Because of the petal size, fabrication in the Georgia Tech main machine shop was difficult. In fact, special jigs had to be built, and even with these jigs, petals were not fabricated to exact dimensions. Therefore, after all petals were cut and milled, the two four-tier assemblies of parallel plates were erected in the main machine shop using custom fitting where necessary. When an assembly was completely erected, an identification code was stamped into each petal. Pop rivets spaced 15.2-cm (6 in.) apart along the lap joints held the assembly together. Plastic rods with 3.8-cm (1.5 in.) diameters maintained the 45.6-cm (18 in.) separation distance. Threaded nylon screws joined the plastic rods together through the metal plates.

After fitting each assembly together in the machine shop, the plates were disassembled, and the individual petals were primed and then given two coats of off-white paint. All 85 petals were then delivered to their final location. The identification code stamped in each petal was used to guide their reassembly into 2 identical waveguides. A 61-cm (24 in.) high pedestal served as the base for each assembly. The pedestal consisted of a center post with eight radial panels. These panels were positioned under the lap joints in the bottom plate. Attachment to the plastic spacer rods was provided by threaded nylon bolts. The bottom plate and the pedestal are electrically isolated from one another. Large-head bolts in the bottom of each pedestal panel provide for leveling the assembled waveguides. Steel cables with turn-buckle adjusters were attached between pedestal panels at lower, outside corner positions to add rigidity to the assemblies. A drawing of the support pedestal is shown in Figure 4.

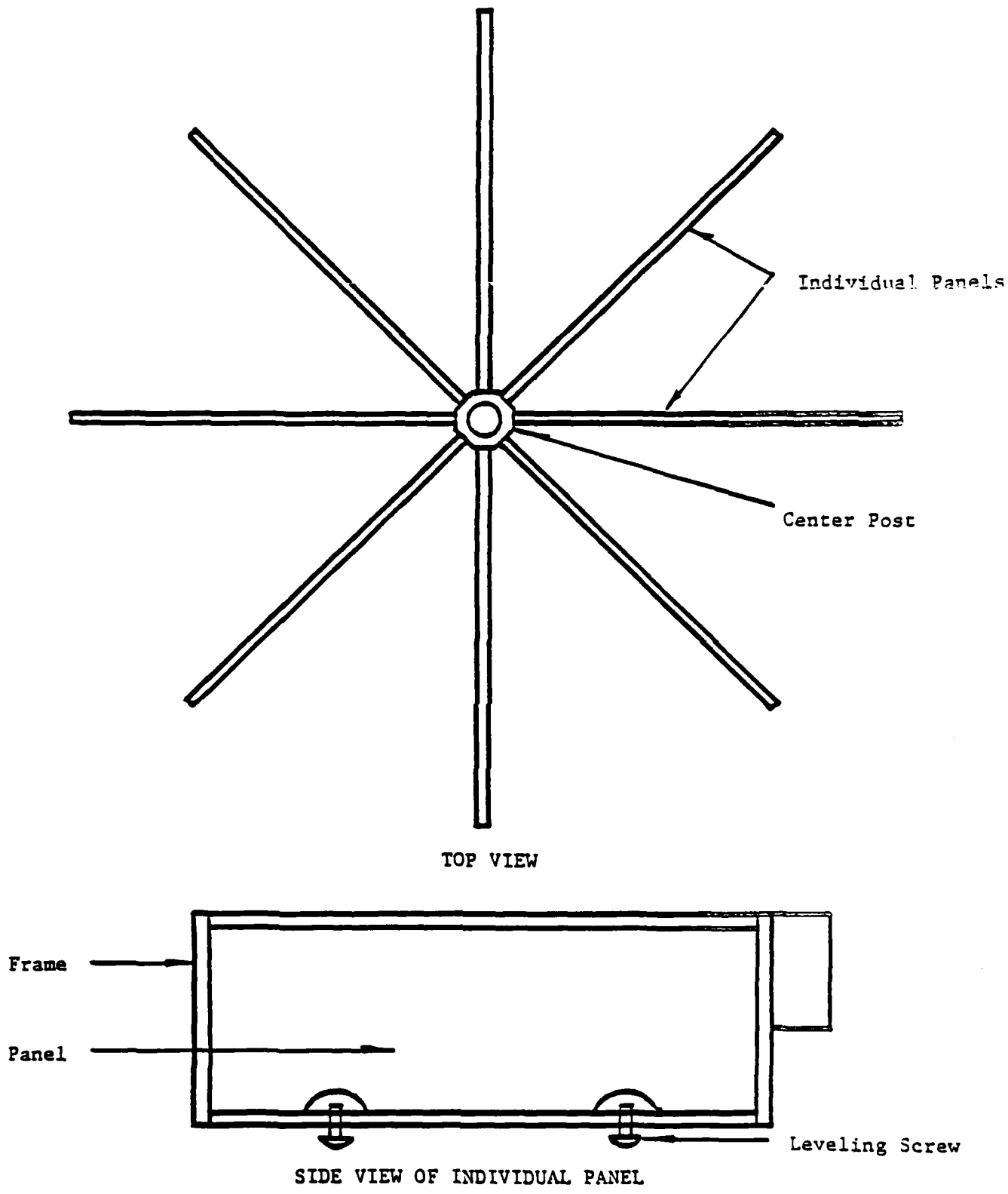


Figure 4. Pedestal used to support circular, parallel-plate waveguides.

## Slotted-Cylinder Antenna

As noted in Section II, the slotted-cylinder antenna was constructed using a 2.44-m (8 ft) long, 10-cm (4 in.) diameter aluminum cylinder with a wall thickness of 0.3175 cm (0.125 in.). The cylinder was cut into four individual sections, two 76.2-cm (30 in.) long and two 45.7-cm (18 in.) long. Slots for the antenna were cut the desired length along the axial dimension of these sections. The two longer sections provided the feed antennas for the upper and lower pairs of plates within the waveguide assembly. For the upper antenna, 45.7 cm (18 in.) of the cylinder section was positioned between the two plates making up the top-most waveguide, and 30.5-cm (12 in.) extended above the upper plate to facilitate installation of the feed cables, baluns, and connectors. For the lower antenna, 45.7 cm (18 in.) of the cylinder section was positioned between the two plates making up the bottom waveguide, and 30.5-cm (12 in.) extended into a nylon insert in the center of the support pedestal. The two 45.6-cm (18 in.) long sections provided the feed antennas for the two internally located waveguides in the four-tier assembly.

The 4 individual sections of the slotted-cylinder antenna, joined by press-fitting nipples are shown in Figure 5. Assembly of the antenna sections involved gently pressing one cylinder section onto the nipple of the lower antenna to achieve a tight fit. Each pair of cylinder sections were joined at the plane of the circular plates. To assure that there was no wave propagation inside the cylinder (and therefore no electrical interference between adjacent waveguides), the top of each nipple was sealed by a metal plate isolator. Holes were provided in the isolator to allow passage of transmission lines. The presence of nipple inserts inside the slotted-cylinder antenna altered the impedance somewhat; however, the baluns/transformers and tuning stubs were adjusted to compensate for this alteration.

Excitation of the slotted-cylinder antenna was done by attaching twin-lead cables across the slots in each of the 4 antenna sections. The cables were routed from the ceiling of the radiation room down through the center of the aluminum cylinder. Attachment across the 4 slots required a mechanically strong connector capable of providing good electrical contact between the

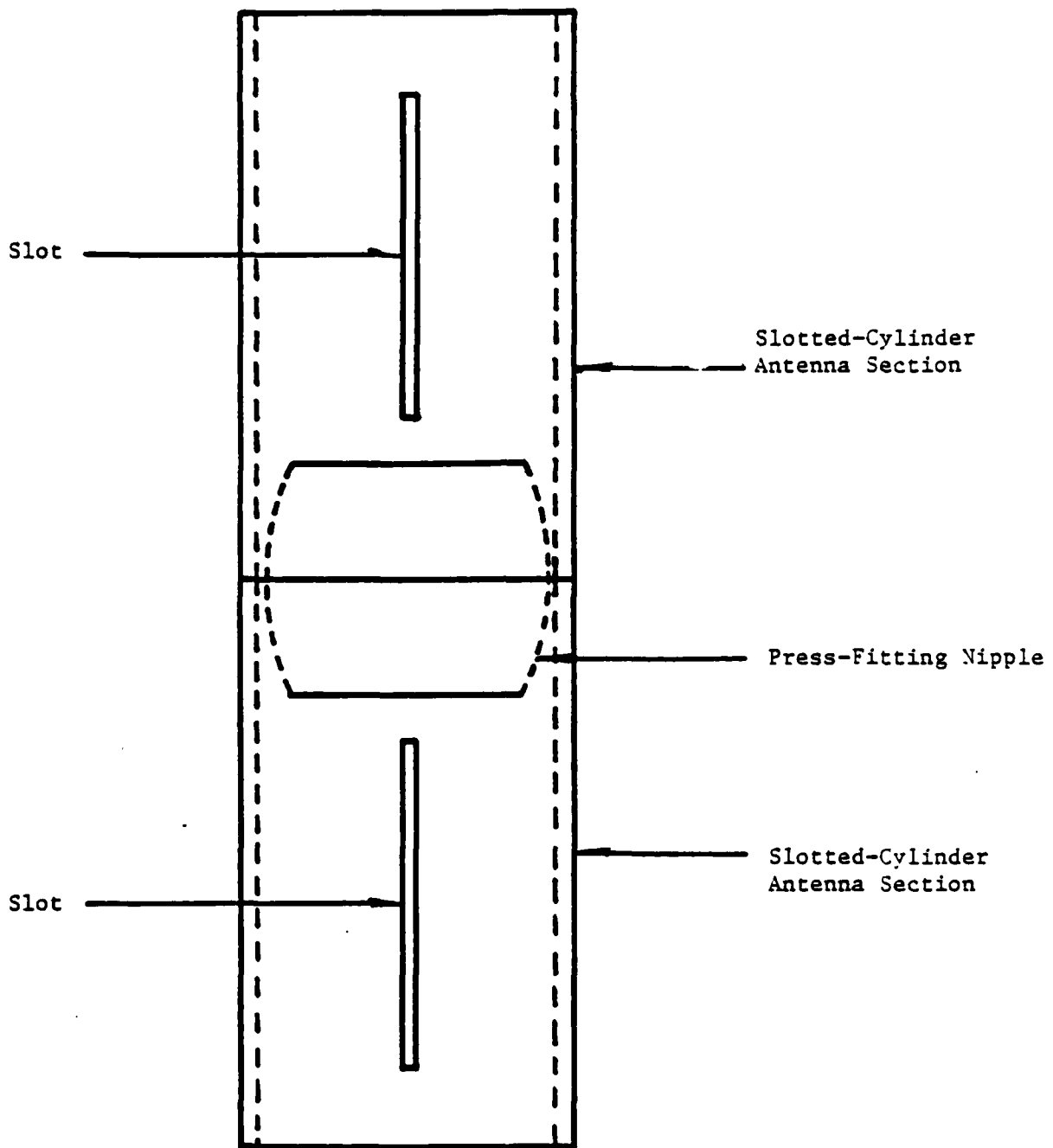


Figure 5. Technique used to assemble slotted-cylinder antenna.

twin-lead cables and the slots. Also, it was important that the connectors not introduce excessive stray capacitance or inductance. The connectors provided for this purpose are shown in Figure 6. Construction of the connectors involved cutting sectoral sections out of nylon block and mounting them across the slots with flat-head screws. Advantages of the nylon material included its transparency to 435-MHz fields and its mechanical strength. Holes were drilled into the nylon block to accept the twin-lead transmission lines from the baluns/transformers. Setscrews were then used to make the electrical connection between the cylinder walls and transmission lines.

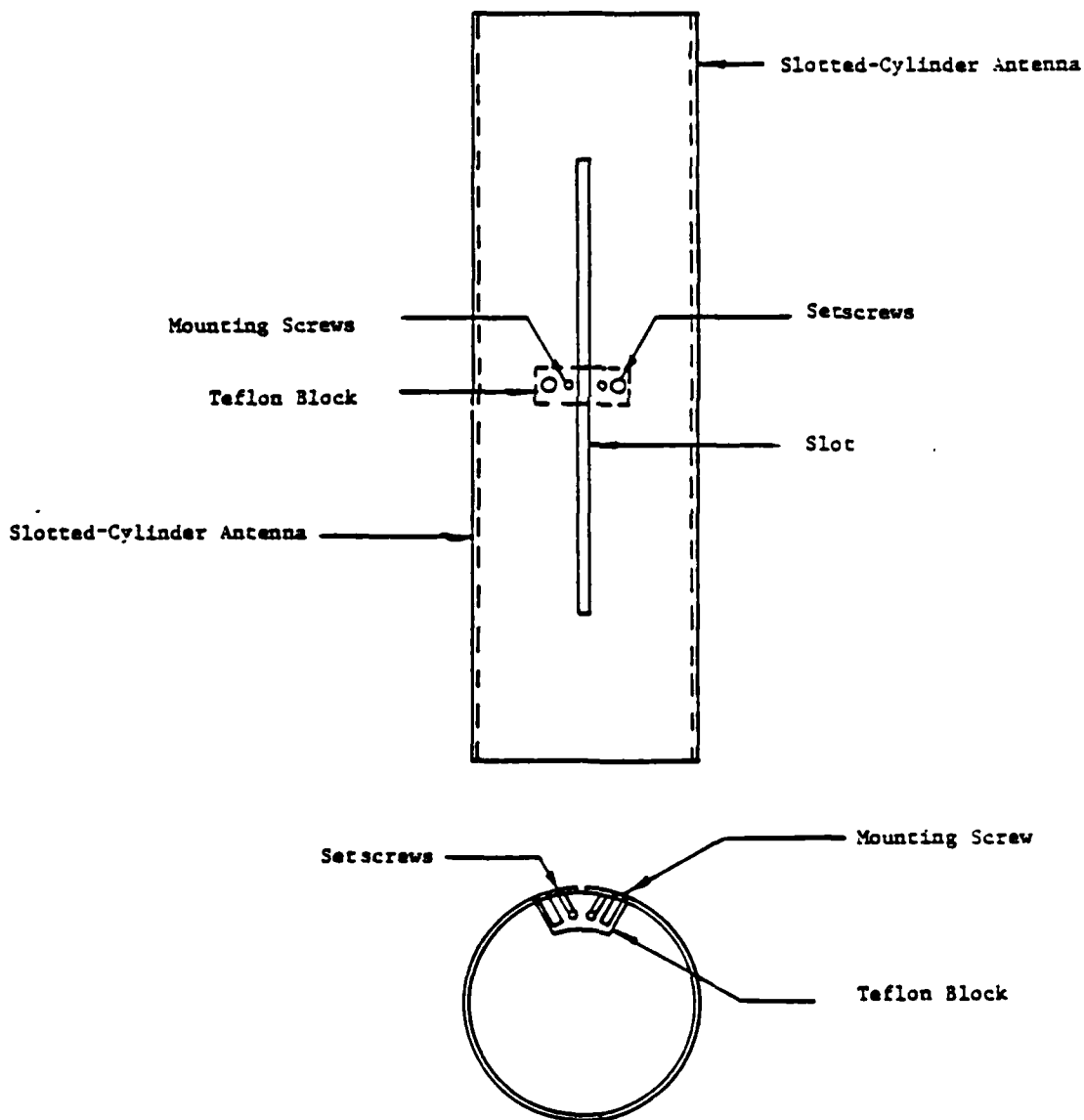


Figure 6. Technique used to mount cables to slotted-cylinder antenna.

#### IV. TRANSMITTER SYSTEM

The transmitter provided for the RFR facility is a Model R9DAT unit purchased from Microwave Control Company (MICON) of Bricktown, New Jersey. The unit is designed as a research transmitter capable of running in either of two modes to provide PW or CW RF outputs at a fixed frequency of 435 MHz. Four separate outputs (one for each circular, parallel-plate waveguide) are provided on the unit top. The power level at all 4 outputs is adjustable by means of 1 front panel control. In Mode 1, the transmitter provides a CW output of up to 200 W average at each of the 4 outputs. In Mode 2, a PW output of up to 5000 W peak is provided at each of the 4 outputs. Other front panel controls allow the pulse width to be varied from 0.25 to 10  $\mu$ s and pulse repetition frequency to be varied from 1.0 to 5.0 kHz. Primary power is also applied by the operation of circuit breakers on the front panels.

##### Transmitter Subassemblies

A photograph of the MICON Model R9DAT Transmitter is shown in Figure 7. The transmitter is made up of 8 major subassemblies mounted in a single equipment cabinet. The 8 subassemblies are evident in Figure 7, and from the top down, they are identified as:

- the Circulator Load Subassembly,
- the #1 and #2 Power Amplifier Subassembly,
- the #1 and #2 Driver Amplifier Subassembly,
- the System Control Subassembly,
- the Oscillator, Preamplifier, and Modulator Subassembly,
- the High Voltage Power Supply Subassembly for #1 and #2 Driver Amplifiers,
- the High Voltage Power Supply Subassembly for #1 Power Amplifier, and
- the High Voltage Power Supply Subassembly for #2 Power Amplifier.

These subassemblies are shown in Figure 8, and a brief description of each is provided in the following paragraphs.

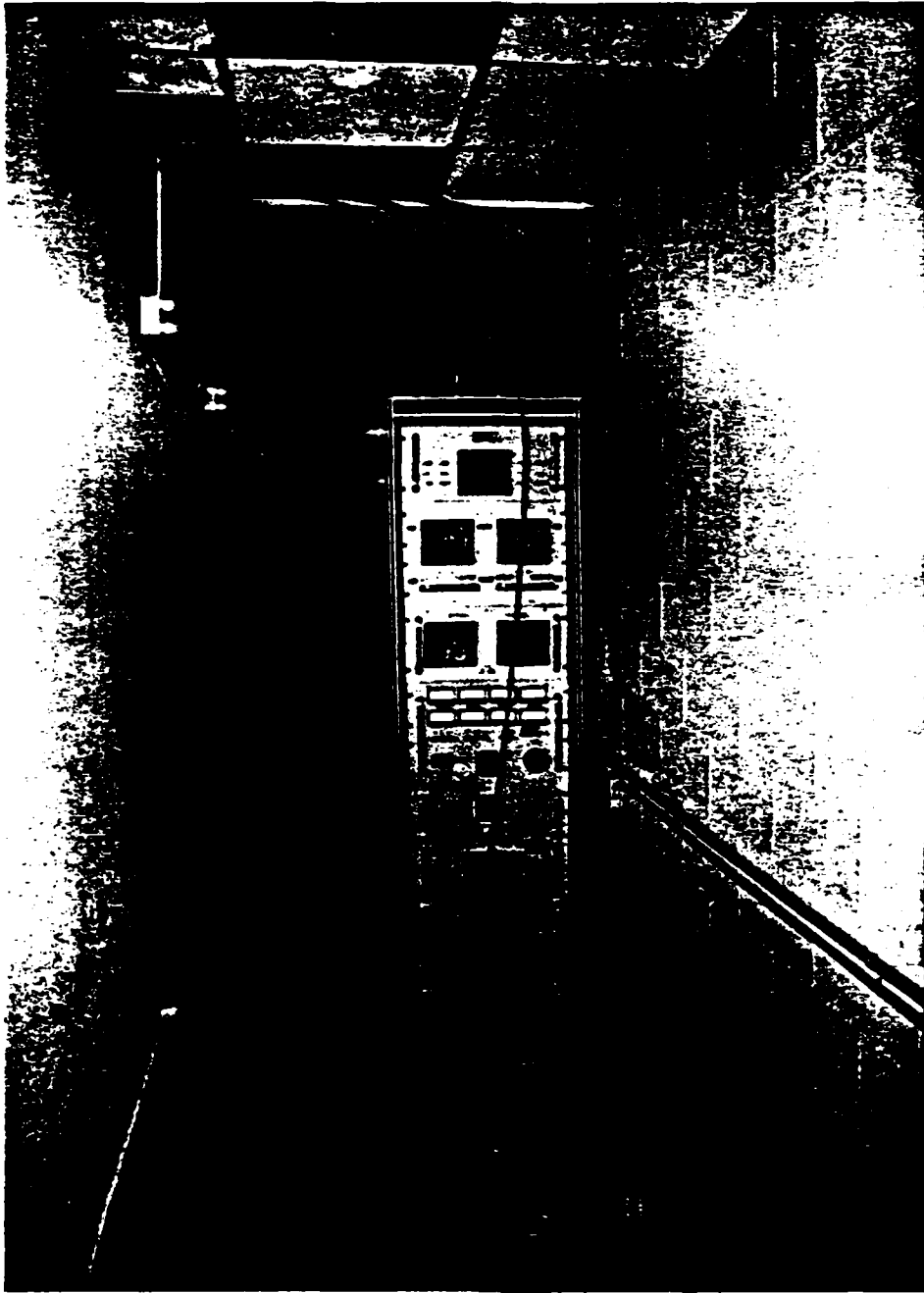


Figure 7. Photograph of MICON Model R9DAT Transmitter.



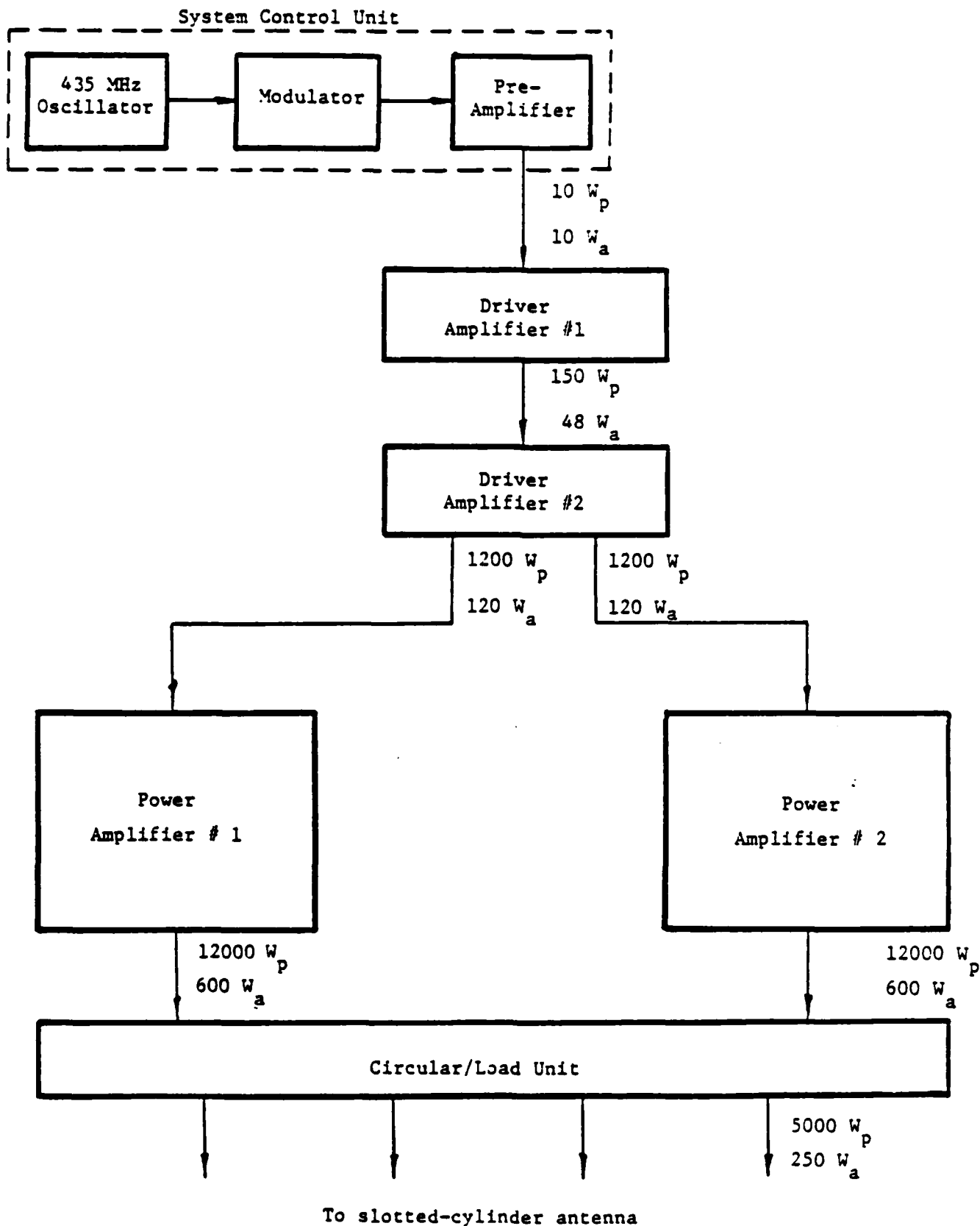


Figure 8. Block diagram of MICON Model R9DAT Transmitter.

### High Voltage Power Supply Subassemblies for #1 and #2 Power Amplifiers

These 2 identical subassemblies provide the high voltages necessary for the 2 output power amplifiers. Front panel controls on each subassembly include a main circuit breaker, status indicator lamps, and a current overload/reset switch. The power supplies contain an overcurrent monitoring circuit that prevents excessive current drain during operation. After any overcurrent situation has been corrected, the reset switch may be momentarily actuated manually to resume operation. Each supply is cooled by a fan whose input is a screened opening on the front panel.

### High Voltage Power Supply Subassembly for #1 and #2 Driver Amplifiers

The high voltage power supply for both of the driver amplifiers is contained in this subassembly. Front panel controls include circuit breakers, status indicator lamps, an overcurrent/reset switch, and test points. The indicator lamps show operate, standby, and overcurrent conditions for each power supply. A manual momentary actuation of the reset switch is necessary for operation of the power supplies after the cause of an overcurrent condition has been cleared. The test points monitor current provided by each supply, with 1.0 V equal to 100 mA of output current. Cooling for the subassembly is provided by a fan whose screened input is located in the front panel center.

### Oscillator, Preamplifier, and Modulator Subassembly

The subassembly provides the solid-state devices and functions necessary to excite the driver amplifier subassembly. Three main controls are provided on the panel, 2 that enable the operator to control pulse width and pulse repetition frequency, and a third that permits either internal or external modulation to be selected. Two coaxial connections are available: one to provide output synchronization pulses, and one to provide an input for external modulation. Under normal operations, the output of this subassembly is about 10 W average in either the PW or CW mode. Cooling is provided by a single fan whose screened input is located on the front panel.

### System Control Subassembly

The subassembly, as its name implies, contains all of the controls

necessary to run the Model R9DAT Transmitter in any of its modes. Eight meters (2 for each of the 4 RF outputs) provide a continuous indication of each RF output by displaying approximate forward and reflected power levels. For meters indicating forward power, the full-scale reading is about 200 W and 5000 W, respectively, in the CW and PW modes. Meters indicating reflected power display a VSWR of 2:1 at full scale for both CW and PW operation. If any one of the 4 outputs present a VSWR in excess of 2:1, a VSWR monitor automatically disables all high voltage power supplies. Also, at the end of a 10-s time period during which the excessive VSWR condition continues to exist, normally-open relay contacts operate to signal an external auto-dialer mechanism (not provided) to call assigned telephone numbers. Other controls on the front panel permit the transmitter to be placed in either the standby or operate mode, and to be manually reset after any overcurrent condition. A switch to permit selection of either CW or PW operation and a RF output control are also provided on the front panel. Indicator lamps on the front panel reflect the overall status of transmitter operation. A fault analyzer is also part of this subassembly, and de-energizes the transmitter if preset conditions at selected monitor points are exceeded. Another set of contacts is provided in the subassembly to permit de-energizing of the transmitter if the RFR room is entered when radiation is underway. Operation of these contacts energizes a Sonalert in the subassembly, and a loud tone is emitted for about 2 min. At the end of 2 min, the auto-dialer mechanism is operated and a sequence of telephone numbers is called. To re-establish normal operation, the monitor in the RFR room must be reset and the reset switch on the system control subassembly must be momentarily actuated manually. An additional overcurrent protection monitor is provided in this subassembly to protect the transmitter from excessive current drain. Like the RFR room monitor, this overcurrent protection monitor operates the Sonalert and de-energizes the transmitter.

#### #1 and #2 Driver Amplifier Subassembly

The subassembly accepts the 10 W output of the oscillator, preamplifier, and modulator subassembly, routes it through 2 cascaded amplifiers and a two-way power splitter, and provides outputs for the power amplifier subassembly. At the output of the first driver amplifier, the power levels are about 48-W

average and 150-W peak, respectively, for CW and PW operation. These power levels are amplified to about 275-W average for CW operation and 2750-W peak for PW operation of the second driver amplifier. The output of the second driver amplifier is split such that CW and PW outputs of about 120 W average and 1200-W peak are provided. Cooling for the subassembly is provided by 2 fans with screened openings for air input on the front panel.

#### #1 and #2 Power Amplifier Subassembly

The subassembly contains 2 identical high power cavity amplifiers that provide either CW or PW outputs for the circulator load subassembly. In the PW mode, the maximum output of the subassembly is 12 kW, which is divided in a two-way power splitter to provide in excess of 5-kW peak to each RF output. In the CW mode, the maximum output of the subassembly is 600-W average, which after routing through the two-way power splitter, provides in excess of 250-W average to each RF output. The cavity amplifiers are protected against overtemperature by sensors that de-energize all high voltage if the internal temperature exceeds 100°C. Overtemperature lamps that indicate an overtemperature condition are provided on the front panel. Each cavity amplifier has a cooling fan, and screened openings for air input to these fans are on the front panel.

#### Circulator Load Subassembly

Output power from the power amplifier subassembly is split, monitored, and interfaced with the RF outputs of the transmitter by this subassembly. The power splitting is accomplished in high power, two-way splitters that take the 2 outputs from the power amplifiers and provide 4 outputs. Each of these outputs is routed through a circulator that provides protection against unacceptable changes in load conditions. The circulators provide sampling ports that permit the monitoring of forward and reflected power for each output (8 monitors). Signals from these 8 monitors are accessible on the front panels through 8 coaxial connectors. The output levels of these signals range from 0 to +10 dBm for forward power. Reflected power monitoring is based on a 2:1 VSWR which, if exceeded, de-energizes all high voltage power supplies. The subassembly is air cooled through a screened opening in the front panel.

Besides the 8 major subassemblies, the transmitter requires interconnecting cables. These cables are provided in the equipment cabinet and interconnect the various subassemblies into connectors on the back of individual chassis. Each cable and connector are color-coded to expedite the interconnection of chassis and, where proper, like connectors are keyed so they can not be connected to the wrong point.

Overall performance specifications for the MICON Model R9DAT Transmitter are summarized in Table 1.

**TABLE 1. OVERALL PERFORMANCE SPECIFICATIONS FOR MICON MODEL R9DAT TRANSMITTER**

Frequency	435 MHz
Power output: Mode 1, CW, each of 4 outputs	200 W
Mode 2, PW, each of 4 outputs	5000 W
RF power balance (output-to-output)	$\pm 0.5$ dB
Pulse rise time	0.12 $\mu$ s max.
Pulse fall time	0.2 $\mu$ s max.
Pulse width	0.25-10 $\mu$ s
Pulse repetition frequency	1-5 kHz
RF power adjustment	Max. to -6 dB
Sync output	+5 V at 50 ohms

The subassemblies and cabling described above define the major operational and performance capabilities of the MICON Model R9DAT Transmitter; however, there is an added important capability provided by a device external to the cabinet-mounted subassemblies shown in Figure 7. The capability involves a MICON Model 01A-28-0005 power combiner that accepts as inputs the 4 circulator/load unit outputs on the cabinet top, and provides a single output with PW and CW power levels of 16 kW and 800 W, respectively. The single output can be connected to one of the slotted-cylinder antennas to provide an exposure power density in excess of 10 mW/cm<sup>2</sup> for 25 rodents. In constructing the circular, parallel-plate facility, the third-level slotted-cylinder antenna was provided with high power cables capable of handling the 16 kW<sub>p</sub> and 800 W<sub>a</sub> power levels.

## V. ANALYSIS OF THE ANTENNA, DISTRIBUTION, AND PARALLEL PLATE SYSTEMS

A major effort during this program involved analysis of the antenna, distribution, and waveguide systems. During the second research program, a prototype version of these systems was analyzed in sufficient detail to clearly indicate their feasibility as a radiation facility concept. However, more analyses were necessary to characterize the performance of these systems in their final installation. These analyses were conducted during the third program. The antenna, distribution, and parallel plate systems consist of the following components:

- a four-tier assembly of circular, parallel-plate waveguides,
- the antennas to excite a particular mode of electromagnetic wave propagation,
- the transmission lines required to feed the antennas,
- the impedance matching and current balancing networks in the transmission lines, and
- the connectors/isolating devices for cabling.

To achieve maximal coupling to the experimental animals, the electric field vector must be parallel to the animal's long dimension. Since the experimental animals will be positioned around the circular plate circumference, equipotential lines of the propagating field must form circles concentric about the axis of the plates. This distribution indicates that the parallel-plate radiators must propagate in the  $TE_{10}$  mode. For this propagation mode, the horizontal electric field will exhibit a half-cosine distribution, with the peak midway between each pair of plates. The distribution can be analyzed by comparing a linear electric field distribution with the electric field  $E_1$  expressed as  $E_1 = E_{01}$ , where  $E_{01}$  is a constant, to a  $TE_{10}$  electric field  $E_2$  expressed as  $E_2 = E_{02} \cos\left(\frac{\pi}{2d}z\right)$ , where  $E_{02}$  is a constant,  $2d$  is the plate separation and  $z$  is the vertical displacement ( $z = 0$  midway between plates). The squares of these quantities multiplied by a scaling factor (the inverse of the waveguide impedance  $z_g$ ) yields the power density. For equal linear and cosine distribution power levels, the result is

$$\left(\frac{1}{Z_g}\right) \int_{-d}^d E_{01}^2 dz = \left(\frac{1}{Z_g}\right) \int_{-d}^d E_{02}^2 \left(\cos \frac{\pi z}{2d}\right)^2 dz, \quad (4)$$

which yields

$$\frac{E_{02}^2}{Z_g} = \frac{2E_{01}^2}{Z_g} \quad (5)$$

Thus, it is clear that midway between each set of plates ( $z = 0$ ) and for equal input power levels, the cosine distribution causes the power density to be twice the value for a linear distribution.

The impedance  $Z$  for the  $TE_{10}$  mode wave propagation is given by

$$Z = \frac{\eta}{\sqrt{1-(f_c/f)^2}} \quad (6)$$

where  $\eta$  = the intrinsic impedance of the medium between the parallel plates,  
 $f$  = the operating frequency of the parallel-plate radiator, and  
 $f_c$  = the cutoff frequency of the radiator (328 MHz for a 45.7-cm (18 in.) plate separation distance.

The impedance of a set of parallel plates operating at 435 MHz in the  $TE_{10}$  mode with a 45.7-cm (18 in.) separation distance is 574 ohms. The radiator can be analyzed as radiating into free space; therefore, the normalized reflected power  $|\rho|^2$  can be determined as

$$|\rho|^2 = \left(\frac{574-377}{574+377}\right)^2 = 0.04 \quad (7)$$

The equation indicates that 4% of the incident power will be reflected, and this level was considered quite acceptable for a long-term, low-level radiation facility.

The effect of experimental animals (rats) on waveguide impedance was analyzed by modeling the rats along an equipotential line as parallel dielectric slabs within a parallel-plate capacitor. The combination of rats

and parallel plates yielded a composite dielectric constant (parallel capacitors model). The modeling approach yielded results that were approximate, but the effort involved was much more consistent with the scope of this program than would have been the case if an exact solution had been sought. Assuming an array of 25 rats, each 17.8-cm (7 in.) long, with a dielectric constant of 49, and separated center-to-center by 45.7-cm (18 in.), the effective relative dielectric constant of the array was determined to be 1.61. The waveguide impedance becomes 452 ohms, thereby causing 1.4% of the incident power to be reflected. The low level of reflected power is very attractive.

Analyses also showed that the waveguide with its 45.7-cm (18 in.) plate separation distance could support TM and TEM propagation modes if they were excited. Consequently, care had to be exercised to assure that they were not excited. The impedance for the  $TE_{10}$  and TEM propagation modes were determined to be 248 ohms and 327 ohms, respectively. To excite only the  $TE_{10}$  mode, the slotted-cylinder antenna described in Section II was selected as the feed for the circular, parallel-plate waveguide. The antenna develops an electric field across the narrow dimension of the slot, thereby generating a radiation field polarized such that equipotential lines are concentric circles about the cylinder. The impedances of the 36.83-cm (14.5 in.) slotted-cylinder antenna, when center fed with a balanced transmission line, varied from 700 to 1400 ohms depending on the transmission line and nipples within the line. As a result, the antenna was well matched to the waveguide impedance.

Analysis efforts also indicated that each pair of plates in the tier assembly should be electrically isolated from the other pairs of plates. Without this isolation, electrical interference phenomena could distort propagated fields and result in the different waveguides generating different exposure fields. The circular, parallel plates located internal to the tier assembly were part of 2 different waveguides--the upper plate surface for one waveguide and the lower surface of the same plate for another waveguide. To determine the extent to which the waveguides were electrically isolated, skin depth calculations were made using the expression given by Ramo et al. (14)

$$\delta = \frac{1}{\sigma R_s} \quad (8)$$



where  $\delta$  = skin depth

$\sigma$  = conductivity ( $3.72 \times 10^7$  mho/meter for aluminum) and

$R_s$  = skin resistance ( $3.26 \times 10^{-7} \sqrt{\text{frequency in hertz}}$  for aluminum).

At 435 MHz, the skin depth was found to be  $3.96 \times 10^{-4}$  cm ( $1.56 \times 10^{-4}$  in.). This value was orders of magnitude less than the thickness of any aluminum sheet that would be used to construct the four-tier assembly of circular, parallel plates; therefore, each pair of plates is well isolated from the others.

A possible source of power dissipation in the exposure facility that needed to be analyzed before finalizing the design was attenuation in the parallel plates. The waveguide attenuation/unit length  $\alpha$  for the  $TE_{10}$  mode is given by

$$\alpha = \frac{2R_s f_c^2}{na f^2 \sqrt{1 - \left(\frac{f_c}{f}\right)^2}} \quad (9)$$

where  $a$  = plate separation distance and the other terms are as previously defined (14). The attenuation was calculated to be  $1.735 \times 10^{-6}$  nepers/2.54 cm (1 in.) or  $1.5066 \times 10^{-5}$  dB/2.54 cm (1 in.). Thus, over a plate radius of 182.9 cm (72 in.), the signal will be attenuated only  $1.08 \times 10^{-3}$  dB. Essentially no signal will therefore be lost due to attenuation in the waveguide.

Proper functioning of the slotted-cylinder antenna required that it be fed with balanced currents at a high impedance. Devices used for impedance transformation and current balancing had to be compact since they were to be located inside the 10-cm (4 in.) cylinder that formed the antenna. Also, these devices had to be capable of handling high peak and average power levels. The impedance transforming balun shown in Figure 9 was developed to meet this criterion. The balun ideally consists of a piece of coaxial transmission line with 2 quarter-wavelength slots milled into it at locations  $180^\circ$  displaced from each other. At the end of the slotted coaxial cable, the center conductor -- which has been extended to become one lead in a twin-lead transmission line -- is shortened to one half of the outer conductor by means of a shorting post. The other half of the outer conductor is electrically connected to a lead having the same diameter as the center conductor. The lead, and the center conductor, then form the twin-lead transmission line with

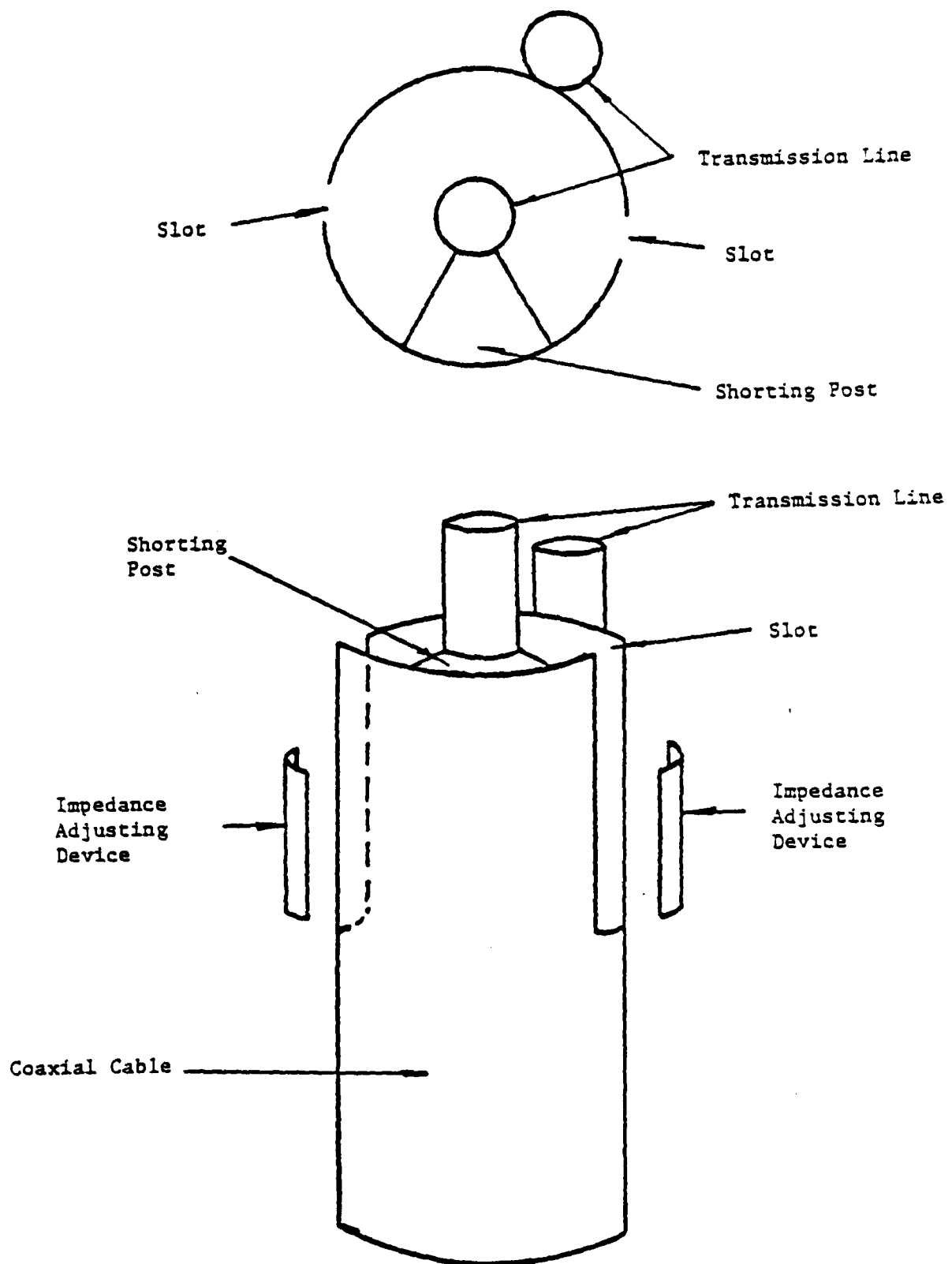


Figure 9. Diagram of impedance transforming balun.

a characteristic impedance of 250 ohms. The twin-lead transmission line was deliberately maintained less than one-tenth wavelength to limit its impedance transforming characteristics and minimize the possibility of undesired stray radiation. Since the twin-lead conductors were electrically separated through the balun by a half wavelength, they were 180° out of phase, and therefore balanced.

In the analysis of impedance transforming baluns, it was noted that the ideal balun may be modeled as two 100-ohm transmission lines in parallel and connected to a coaxial line as shown in Figure 9. One of the two 100-ohm lines is terminated in a short circuit while the other is terminated in a load (ultimately the antenna). If the length  $L$  of each 100-ohm transmission line is one-quarter wavelength, the impedance at their junction with the coaxial cable can be determined. In this case, the short circuit transforms to an open at the junction and the load  $Z_L$  transforms back to become

$$Z_T = \frac{(100)^2}{Z_L} \quad (10)$$

For a matched system,  $Z_T = 50$  ohms, so  $Z_L$  must be 200 ohms. The value is somewhat low and does not provide a good match to the slotted-cylinder antenna. However, if the slot lengths in the balun coaxial cable are shortened slightly by means of metal adjusting devices (see Figure 9), the currents can be kept nearly balanced while the impedance necessary for the best match can be changed markedly. This procedure was used to coarse tune the slotted-cylinder antenna.

The impedance transforming baluns were located inside the slotted-cylinder antennas, and, since they did not provide a perfect match, tuning stubs were used in the signal distribution system exterior to the slotted-cylinder antennas. These open stubs provided an ability to accomplish fine tuning, adjust the match to compensate for aging, and equalize the power transmitted to each pair of parallel plates. These stubs function by cancelling the reactive portion of the transformed impedance at a certain point on the transmission line, thus reducing the magnitude of the impedance discontinuity. Single and multiple stubs were used as necessary to achieve an impedance match such that the reflected power was about 14 dB below the incident power at each waveguide. The stubs were fabricated from open-circuited sections of RG-8

coaxial transmission line. The stubs were connected in parallel with the main transmission line by means of "T" connectors and located above the edge of the parallel plates in the ceiling for convenient access. The open ends of the stubs were protected by tape to a thickness greater than a conductor spacing to prevent the introduction of unwanted capacitances due to the presence of metal objects within their fringing fields.

It was necessary for the exposure facility to function properly with reasonably high levels of average and peak powers. Specifically, 3 of the parallel plate waveguides had to accommodate 200 W of average power and 5 kW of peak power. The fourth parallel plate waveguide had to accommodate 800 W of average power and 20 kW of peak power. Average power limitations were determined by power levels capable of causing thermal destruction of conductors or, more commonly, thermal destruction of dielectrics. Peak power limitations were determined by power levels capable of causing dielectric breakdown (arcing). Our analysis effort noted that a dry air dielectric is excellent for high average powers since it is essentially lossless, but relatively poor dielectric breakdown properties limit its peak power capabilities. Coaxial cables filled with a polyethylene foam dielectric were chosen for the transmission lines since they exhibited superior peak and average power characteristics. These cables can tolerate the highest average powers anticipated with a voltage standing wave ratio of 4.0 without exceeding their power ratings. The impedance transforming baluns have the same power ratings as these cables.

The slotted-cylinder antenna was analyzed to determine its peak power rating. Dry air experiences electrical breakdown under an electric field strength of 30,000 V/cm. The antenna slot was 0.312-cm (0.125 in.) wide. Thus, voltages in excess of 9,525 V would be necessary to cause air in the slot to break down. In a conservative analysis, we assumed that the impedance looking into the slot was 1400 ohms. We further assumed that the potential at the center of the slot was 1.414 times the potential that would have been present if the electric field was uniformly distributed, rather than cosine distributed, along the slot. Under these circumstances, the peak power rating of the slot was determined to be 32.4 kW. Since the cylinder impedance is usually closer to 700 ohms, a more likely peak power rating is 64.8 kW. Both ratings far exceed the power levels the slots will have to withstand.

An eighth-wavelength dipole (15) antenna was used to map horizontal and vertical components of the electric field along the edge of each pair of parallel plates. The purpose of this mapping was to assure that all experimental animals would be exposed to the same environment and the waveguides were operating in the  $TE_{10}$  mode. Measurements of the horizontal field component were also made to establish the existence of a cosine field distribution between the plates of each waveguide.

The horizontal component of the field was found to vary by 2 dB-peak-to-peak around the circumference of the plates. The vertical field electric component was 17 dB down from the horizontal component, thereby confirming TE propagation. The horizontal field component was found to exhibit a half-cosine variation between the plates, and this established the propagation mode as  $TE_{10}$ . The exposure fields of each waveguide were probed to determine whether any interference was distorting the propagated fields. The electric field structure was found to be essentially identical for each set of plates and interference distortion was not observed.

## VI. CAGE CONSIDERATIONS

Cage design and spacing are extremely important, and often overlooked, considerations in bioeffects studies that involve experimental animals exposed to electromagnetic waves. The importance of cage design stems from the fact that it establishes the physical environment for the animal throughout the exposure duration; therefore, it is both a dominant factor in establishing the animal's well being during exposure and an influencing factor in experimental results (16). Cage-to-cage spacing is important because scattered waves from the cage, the animal, or both can introduce uncertainties in dosimetry determinations. The exact extent to which cage design and spacing influence a given study depends on a variety of subjective and objective considerations that interact differently from one study to the next; however, for all studies, it is mandatory that animal cages be designed and positioned with sufficient care to assure that they do not introduce artifactual responses in the study result.

### Cage Design Considerations

For this study, the importance of exposure cages was especially evident in the fact that the animals are to be housed in the cages for extended time periods. Cage design had to be thoroughly considered from the point-of-view of both physical environment and experimental results. Overall, it was important that the cage design--

- involve materials that are visibly transparent to permit easy determination of animal status, electromagnetically transparent to reduce intercage scattering to tolerable levels, and structurally sufficient to provide long-term housing without encouraging gnawing,
- use minimum dimensions to permit the total exposure area to be as small as possible, and
- provide adequate means for ventilation and cleanliness.

Prior to considering specific cage designs, it was necessary to assemble

certain information regarding the rats to be used as experimental and control animals. The primary information of interest to cage design is presented below (17):

- Birth Weight: 5 to 6 g
- Weaning Age: 3 weeks
- Weight at Weaning: 40 to 60 g
- Adult Weight: 400 to 450 g
- Body Temperature: 38.2°C
- Respiration Rate: 65 to 110 breaths/minute
- Adult Metabolism: 130 calories/kilogram/day
- Water Consumption: 35 ml/day
- Food Consumption: 10 g/day
- Urine Excreted: 10 to 15 ml/day
- Feces Excreted: 7 to 14 g/day
- Life Span: 3 years

From this information, we noted that, within about 30 days after birth, young rats are weaned and have attained 20 to 25% of their adult weight. Therefore, the exposure regimen was initiated using 200 experimental and control rats 30 days of age. This regimen eliminated the necessity of using small cages when the rats are young, and then switching to larger cages as the rats matured.

From a physical comfort point-of-view, the primary design considerations were cage dimensions, ventilation, and sanitation. Cage dimensions were important because they govern not only freedom of movement and postural adjustments, but they also influence the area required in the exposure zone. Defining cage dimensions, we noted that rat cages advertised in catalogs typically offer a floor area of about 645 cm<sup>2</sup> (100 in.<sup>2</sup>) and a height of 15.2 cm (6 in.). These dimensions were compared with space guidelines for adult rats (greater than 300 g) as recommended by the National Institutes of Health (18). These guidelines specify a minimum floor area of 258 cm<sup>2</sup> (40 in.<sup>2</sup>) and a cage height of about 17.5 cm (7 in.). A survey of cages in the Georgia Tech and Emory University animal housing facilities revealed that rats are routinely housed for long time periods in cages with a floor area of 452 cm<sup>2</sup> (70 in.<sup>2</sup>) and a height of 17.8 cm (7 in.). After reviewing these various cage

designs and discussing the subject with knowledgeable animal caretakers, we decided that a floor area of 290.3 cm<sup>2</sup> (45 in.<sup>2</sup>) should be adequate for housing the rats throughout their lifetime. The dimensions of this floor area would be 22.9-cm long x 12.7-cm wide (9-in. long x 5-in. wide). These dimensions would permit postural changes to the extent that the rats could turn around in their cages, but they could not comfortably align themselves parallel to the short dimension of the cages. The ability to make these postural changes is important for the physical well-being of the rats, yet the changes are always such that the rat's broadside faces the exposure field source. An internal height of 17.8 cm (7 in.) would be provided; however, the overall height of the cage would be somewhat taller to accommodate waste disposal provisions.

Cage ventilation was important because of the necessity of keeping reasonably constant environmental conditions and promoting animal comfort. Environmental conditions of concern were temperature, humidity, and air movement. Since we anticipated that ambient air would ventilate the cages, it was necessary for the cage design to provide easy entrance and exit of room air. Consequently, the cages were designed with relatively large openings in their sides, tops, and bottoms. These openings provided sufficient air circulation necessary for adequate ventilation.

The final cage design consideration for physical comfort was sanitation, and the primary emphasis was on assuring that feces and urine were not retained in the cages. Any appreciable retention of feces and urine in the cages would mean that the animals could not be kept clean, undesired odors would develop, perturbations could be induced in the exposure field, and the possibility of disease would be substantially increased. In view of this consideration, the cage design had to provide a means by which feces and urine could drop through the floor and then be externally disposed of. This design required cage floors to be constructed of nonabsorbent materials with the structural ability to support the rats while providing large and frequent openings. If later biological examinations were to require collection of feces and/or urine, non-perturbing collectors can be provided below the cage and outside the exposure field.

When materials for the cage design were considered, we noted that Plexiglas, polypropylene, polycarbonate, Styrofoam, polystyrene, and glass



have all been used to house individual or groups of experimental animals. Polycarbonate is the generic designation for a tough, transparent thermoplastic characterized by high impact strength and high softening temperature. Its optical and thermal properties are essentially those of glass, and it can be autoclaved. Similarly, polypropylene is the generic designation for various translucent thermoplastic fibers. These plastics or fibers are polymers of propylene and can be autoclaved. Polystyrene is a rigid, transparent thermoplastic with good physical and electrical insulating properties, and finds its primary usage in molded products and foams. Plexiglas is a tough, rigid, acrylic plastic that is visibly transparent and available in sheet form. Styrofoam is an expanded form of polystyrene plastic, and is neither transparent nor particularly tough. Except for Styrofoam, these materials are chemically resistant and may be drilled or machined to fit laboratory specifications.

Of these materials, the ones most commonly used for housing animals during studies involving electromagnetic exposure are Plexiglas and Styrofoam. The rigidity and visible transparency of Plexiglas results in its being an attractive material for cage design; however, at S-band frequencies and above, it introduces scattering of the exposure field and thereby complicates dosimetry efforts (19). Joining Plexiglas panels to form cages is a simple matter because of the availability of glues designed for that specific purpose. Styrofoam is the only cage design material that is, for all practical purposes, electromagnetically transparent regardless of frequency. However, when rodents are used as experimental animals, Styrofoam is generally useful only for short-term studies because it is easily gnawed. Styrofoam panels can be readily joined to form cages provided glues with organic solvents are not used. If glues with organic solvents are used, the Styrofoam is solubilized and the joint is destroyed.

When the relative advantages and disadvantages of these various materials were analyzed, two different cage designs using Plexiglas and Styrofoam were considered. Frequency was not a concern in either of the designs because, over the 420-to-450 MHz range, both Plexiglas and Styrofoam are electromagnetically transparent. The first design used Styrofoam and glass as the cage materials, and was patterned after the design of Catravas (20). A prototype cage was constructed using 5-cm (2 in.) thick sheets of

commercially available Styrofoam cut into panels as shown in Figure 10. The 5-cm (2 in.) thickness was selected in anticipation of gnawing by the rats; however, to minimize this gnawing, the interior surfaces of the Styrofoam panels were coated with quinine as a 10% solution in absolute methanol. Quinine is very bitter and therefore unpleasant to taste. Further, it is nontoxic to rats and experimental efforts showed the coated panels did not influence 450-MHz electromagnetic fields. The coated panels were joined together using casein glue to form a cage with internal dimensions of about 22.9-cm (9 in.) long, 12.5-cm (5 in.) wide, and 17.8-cm (7 in.) high. Glass rods with 0.635-cm (0.25 in.) diameters were spaced 1.25 cm (0.5 in.) apart to form the cage bottom and 2.54 cm (1.0 in.) apart to form the cage top. These rods were supported in position by pressing them into the soft Styrofoam panels. A large male rat was housed in the cage for 4 months to observe postural adjustments and gnawing tendencies. Dry food was provided ad libitum and water was available in a conventional water bottle mounted on the cage top.

After 4 months of observations, the following conclusions were reached:

- The cage appeared to be of adequate size, and the rat seemed to be physically comfortable.
- Initially, there seemed to be some discomfort with the glass rods in the cage bottom. This discomfort appeared to be due to difficulty in maintaining footing. After the first day or so, the rat seemed to adjust to these rods and no further evidence of footing difficulty was observed. However, before initiating a multi-year bioeffects study, other designs for the cage bottom should be considered. One possible design might be to position the glass rods perpendicular, rather than parallel, to the long dimension of the cage. We observed that the glass rods were quite adequate for providing removal of feces and urine.
- Gnawing of the Styrofoam panels was minimal, indicating that the quinine-methanol solution was effective in deterring the rat's tendency to chew out of the cage.
- The opaque characteristic of Styrofoam made it difficult to readily observe the rat. This difficulty would be a matter of appreciable

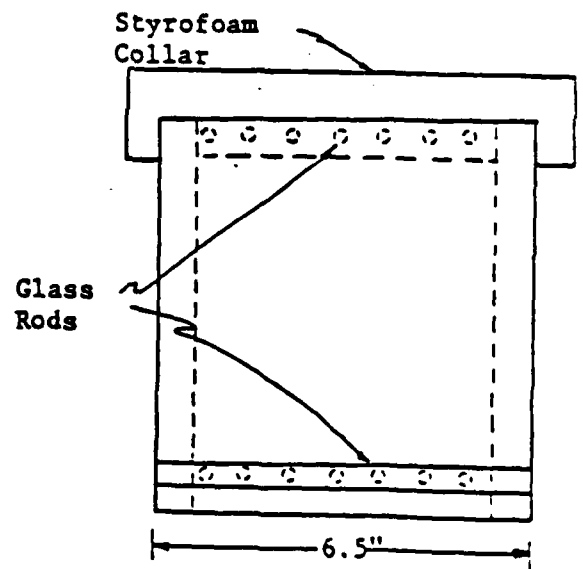
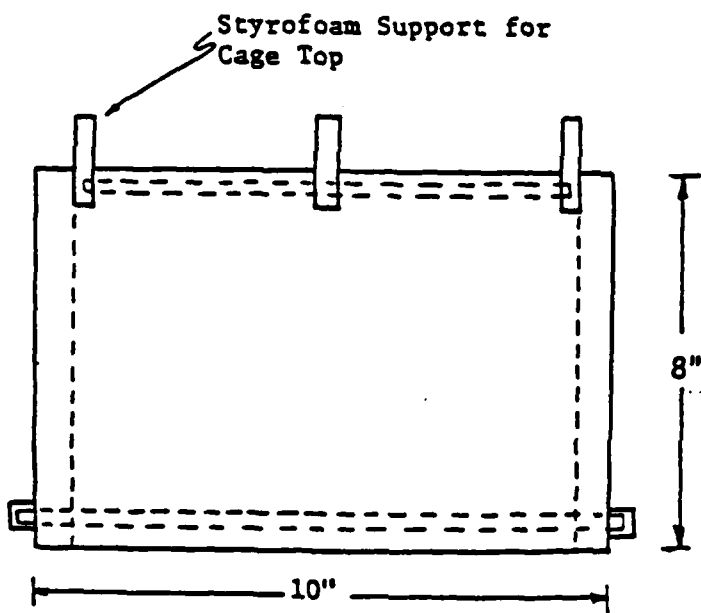
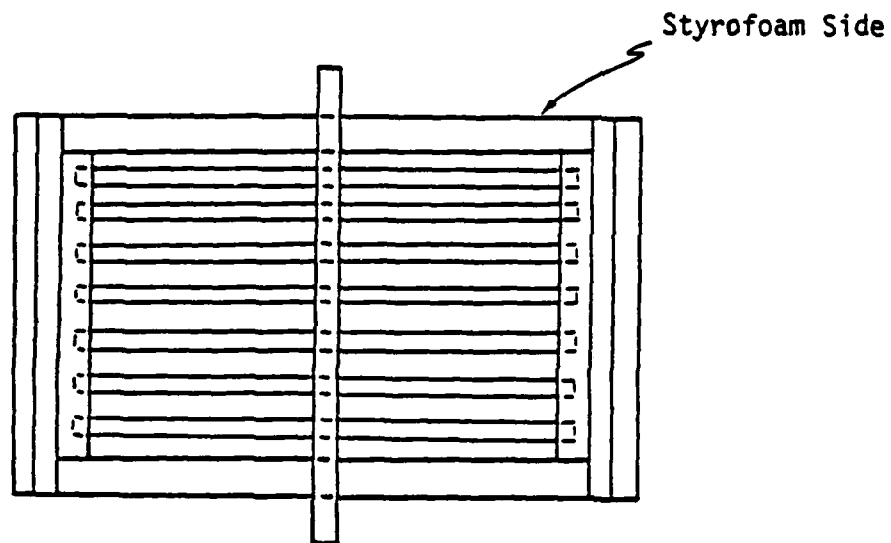


Figure 10. Styrofoam cage design for housing rats during continuous electromagnetic radiation exposure.

concern with 200 rats that must be individually observed on a frequent basis.

The conclusions reached as a result of experience with the Styrofoam and glass cage led to the analysis of a second cage design. For this analysis, the overall cage shape and internal dimensions were essentially identical to those of the first design; however, the Styrofoam material was replaced by Plexiglas with a 0.635-cm (0.25 in.) thickness. Earlier evaluations had been conducted to determine the scattering characteristics of Plexiglas at 430 MHz (19). These evaluations involved transmitting and receiving antennas positioned 3 m (10 ft) apart in a shielded, anechoic chamber. The transmitting antenna was connected to a high power signal source and the receiving antenna was routed to a power meter. The signal source output was adjusted to yield a convenient reading on the power meter. Then, without changing either the signal source or power meter, Plexiglas sheets were positioned between the 2 antennas. Each sheet had an area of 0.84 m<sup>2</sup> (9 ft<sup>2</sup>) and sheets of two different thicknesses -- 0.635 cm (0.25 in.) and 0.952 cm (0.375 in.) -- were used. The position of the sheets between the antennas was varied from directly in front of the transmitting antenna to a location directly in front of the receiving antenna. No detectable change in power meter reading was observed at 430 MHz for either of the Plexiglas sheets or for any position between the antennas. We therefore concluded that in the 420-to-450 MHz frequency range, Plexiglas sheets with thicknesses up to 0.952 cm (0.375 in.) would not introduce intolerable perturbations in the exposure field; consequently, these Plexiglas sheets were an acceptable cage design material for this study.

The Plexiglas cage design that evolved is shown in Figure 11. This design used 0.635-cm (0.25 in.) thick Plexiglas for 3 sides, the food hopper, and the soil tray. The top and fourth side were constructed of 0.952-cm (0.375 in.) thick Plexiglas. The thicker Plexiglas on the fourth side was necessary to provide a grating through which the caged animals could access food. The food hopper held a supply of pellets sufficient for several days. The hopper grating was constructed using 3-mm-diameter glass rods mounted vertically on 1.113-cm (0.4375 in.) centers through an opening or window in the thicker cage side. The arrangement allowed the caged animals to feed at will.

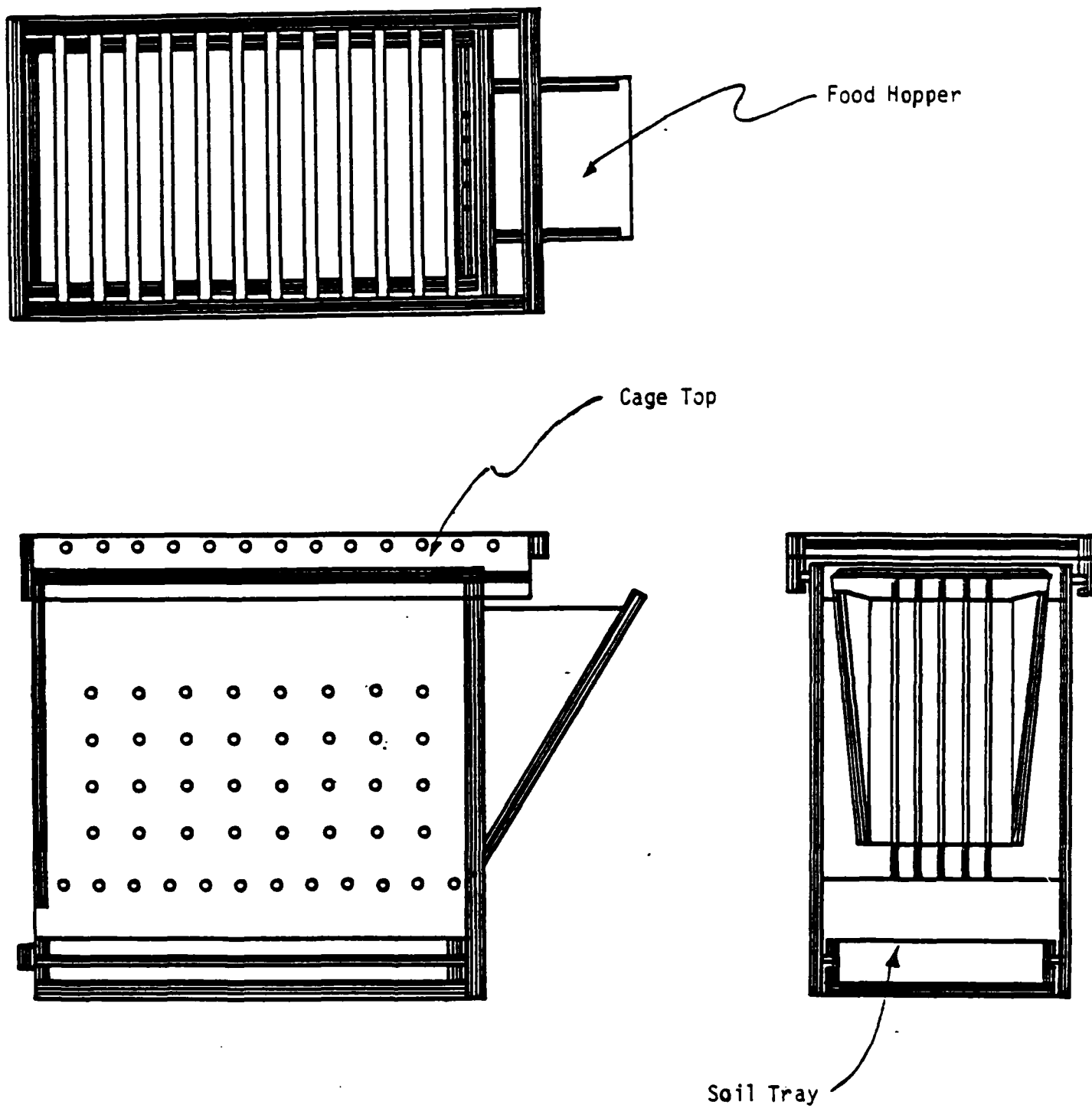


Figure 11. Plexiglas cage for housing rats during continuous radiation exposure.

Six-millimeter-diameter glass rods mounted parallel to the transverse axis of the cage on 1.905-cm (0.75 in.) centers formed the cage bottom. These rods permitted animal waste to drop through the cage onto a soil collection tray for later disposal or study, as appropriate. The technique reduced the number of times the entire cage had to be washed to perhaps once/week, and thus extended the useful life of the cages. However, the soil trays had to be cleaned as often as necessary to maintain satisfactory levels of cleanliness and odor control.

Water for animals in the cages was provided by individual water bottles. These bottles used glass rather than metal sipper tubes to minimize field perturbations that may affect power exposure and absorption (21). To determine the relative effect of water-filled glass and metal sipper tubes on the exposure field, a small dipole antenna was imbedded in the nose of a body of phantom modeling material shaped as shown in Figure 12 to simulate a rat. The antenna was connected to the input of a power meter which served as a relative power indicator. The simulated rat was then irradiated with a 450-MHz field and relative power indications were noted as a function of various sipper tube conditions. The conditions and associated test results are presented in Table 2. The test results indicate that, if a sipper tube (either metal or water-filled glass) was positioned parallel to the direction of propagation of the incident exposure field, the power coupled to an animal drinking from the water bottle was likely to increase. The increase for a metal sipper tube was profound, while only a slight increase occurred if a water-filled glass sipper tube was used. No power increase (and even a slight reduction) occurred when the sipper tube was oriented perpendicular to the direction of propagation of the incident exposure field.

Since water bottles for cages used with the circular parallel-plate radiation facility could use glass sipper tubes and also be oriented perpendicular to the exposure field, no perturbations associated with water provisions occurred over the frequency range of 420 to 450 MHz.

For a chronic study of radiofrequency radiation effects on rodents, concern arose regarding the possible interaction between the exposure field and the dry pellets normally used as food. To determine whether such an interaction would occur in the frequency range of 420 to 450 MHz, small transmitting and receiving antennas were set up. The receiving antenna was connected to a

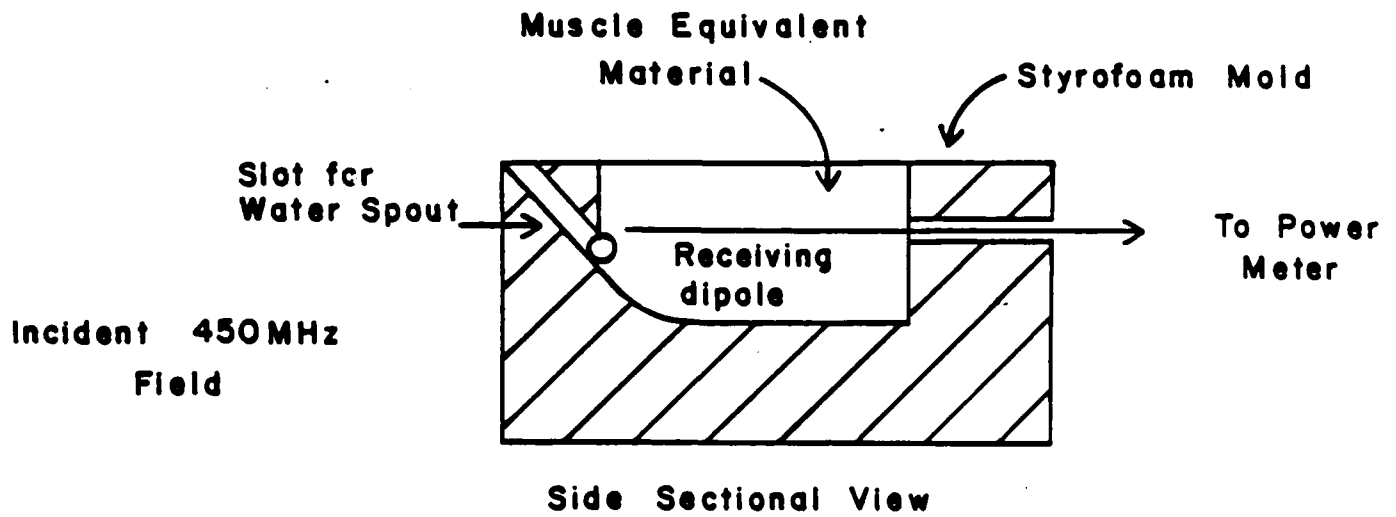
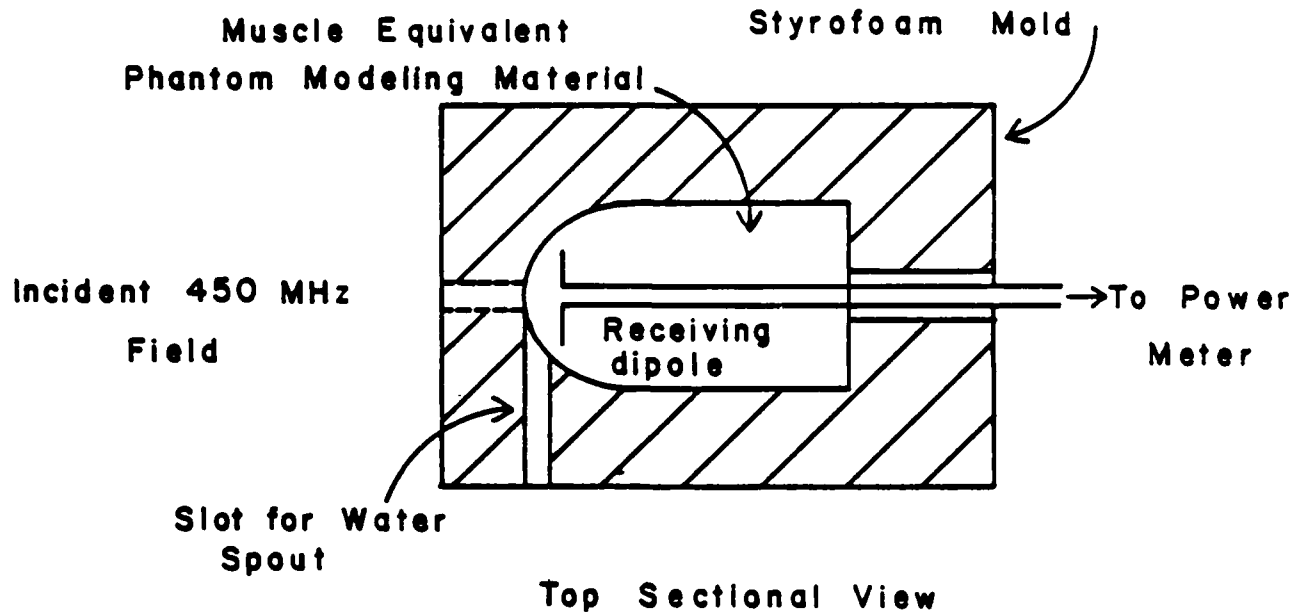


Figure 12. Model used to evaluate effect of exposure field on watering provisions.

TABLE 2. RESULTS OF MEASUREMENTS TO DETERMINE EFFECTS OF EXPOSURE FIELD ON WATER PROVISIONS.

Orientation of Receiving Antenna	Water Spout	Orientation of Water Spout	Relative Power Indicator
			no spout      spout present
Parallel to Exposure Field	Metal	Parallel to Exposure Field	36 $\mu$ W      151 $\mu$ W
		Perpendicular to Exposure Field	36 $\mu$ W      32 $\mu$ W
	Water-Filled Glass	Parallel to Exposure Field	36 $\mu$ W      46 $\mu$ W
		Perpendicular to Exposure Field	36 $\mu$ W      36 $\mu$ W
Perpendicular to Exposure Field	Metal	Parallel to Exposure Field	4.4 $\mu$ W      ~ 0 $\mu$ W
		Perpendicular to Exposure Field	4.4 $\mu$ W      3.4 $\mu$ W
	Water-Filled Glass	Parallel to Exposure Field	4.4 $\mu$ W      3.8 $\mu$ W
		Perpendicular to Exposure Field	4.4 $\mu$ W      2.9 $\mu$ W



power meter adjusted to read on a sensitive, low power scale. With nothing between the antennas, the signal source feeding the transmitting antenna was adjusted to provide a reference level on the power meter. Increasingly large amounts of dry food pellets were then introduced between the 2 antennas while the power meter indication was observed. With food quantities far in excess of what would ever be used in an individual cage, there was no change in the reference level on the power meter. We therefore concluded that the food pellets would not perturb an exposure field in the frequency range of 420 to 450 MHz.

Body weight and core temperature analyses were conducted concurrently for the purpose of comparing, as a function of time, rats housed in the new Plexiglas cages with rats housed in conventional metal cages. Growth rate and body temperature were considered important indicators of overall health status, and, if rats housed in the two different type cages experienced different growth rates and/or core temperatures, features of the Plexiglas cage design would need to be reconsidered. A metal cage rack complete with 10 conventional metal cages was obtained and 10 Plexiglas cages were constructed with the glass rods in the cage bottom positioned parallel to the cage long dimension. Twenty male Sprague-Dawley rats were obtained from Emory University and arbitrarily divided between the two types of cages. Both groups of caged rats were housed adjacent to each other in the same room, with food and water provided ad libitum. Body weight and core temperature were measured daily (except Saturday and Sunday) as the rats grew from about 110 g to about 170 g. The resulting data are shown in Figures 13 and 14. An analysis of these data concluded that housing rats in Plexiglas cages introduced no biological differences that would not have occurred if the rats were housed in conventional metal cages. Therefore, the Plexiglas cages would be satisfactory for RFR studies.

Concurrent with the analysis of body weight and core temperature, rats housed in the Plexiglas cages were observed daily (except Saturday and Sunday) for postural preferences. These observations were made to determine if the direction of the glass rods in the cage bottom influenced whether the rats positioned themselves parallel or perpendicular to the cage long dimension.

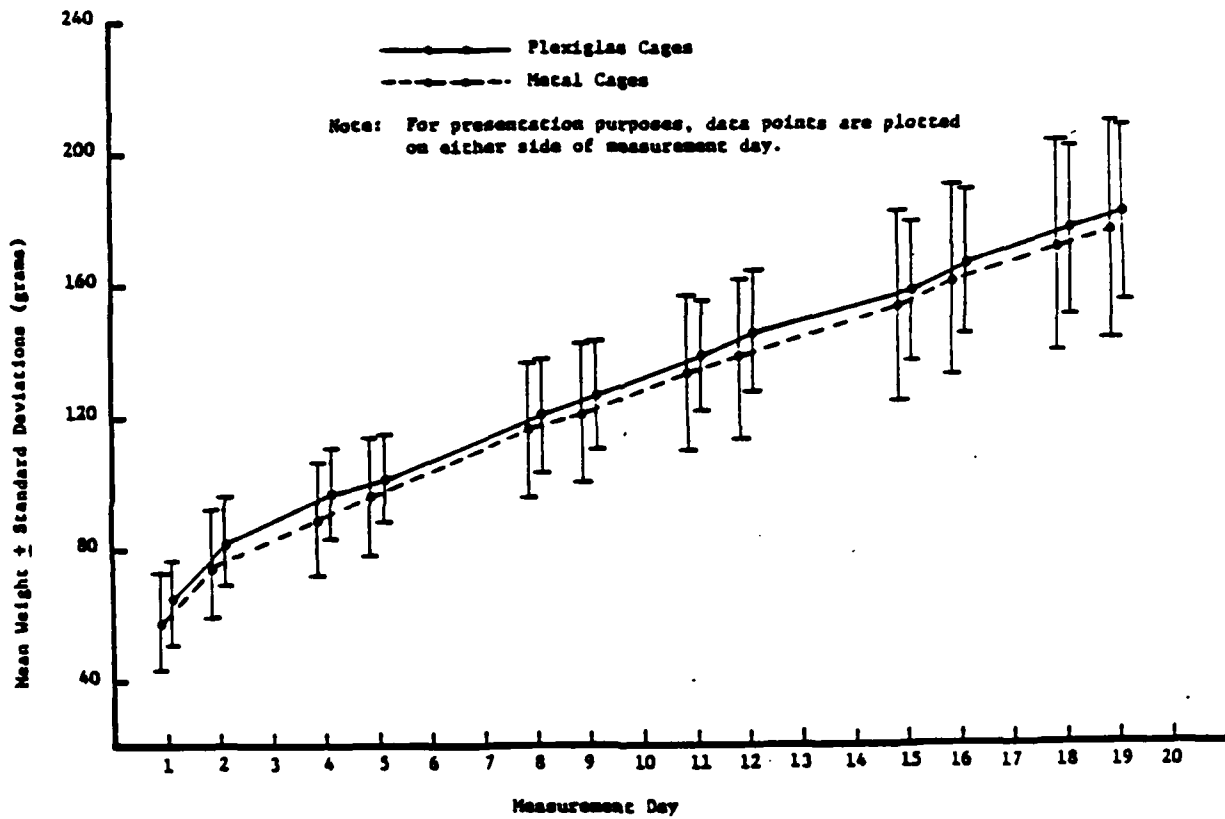


Figure 13. Comparison of body weight of rats housed in Plexiglas cages to rats housed in standard metal cages.

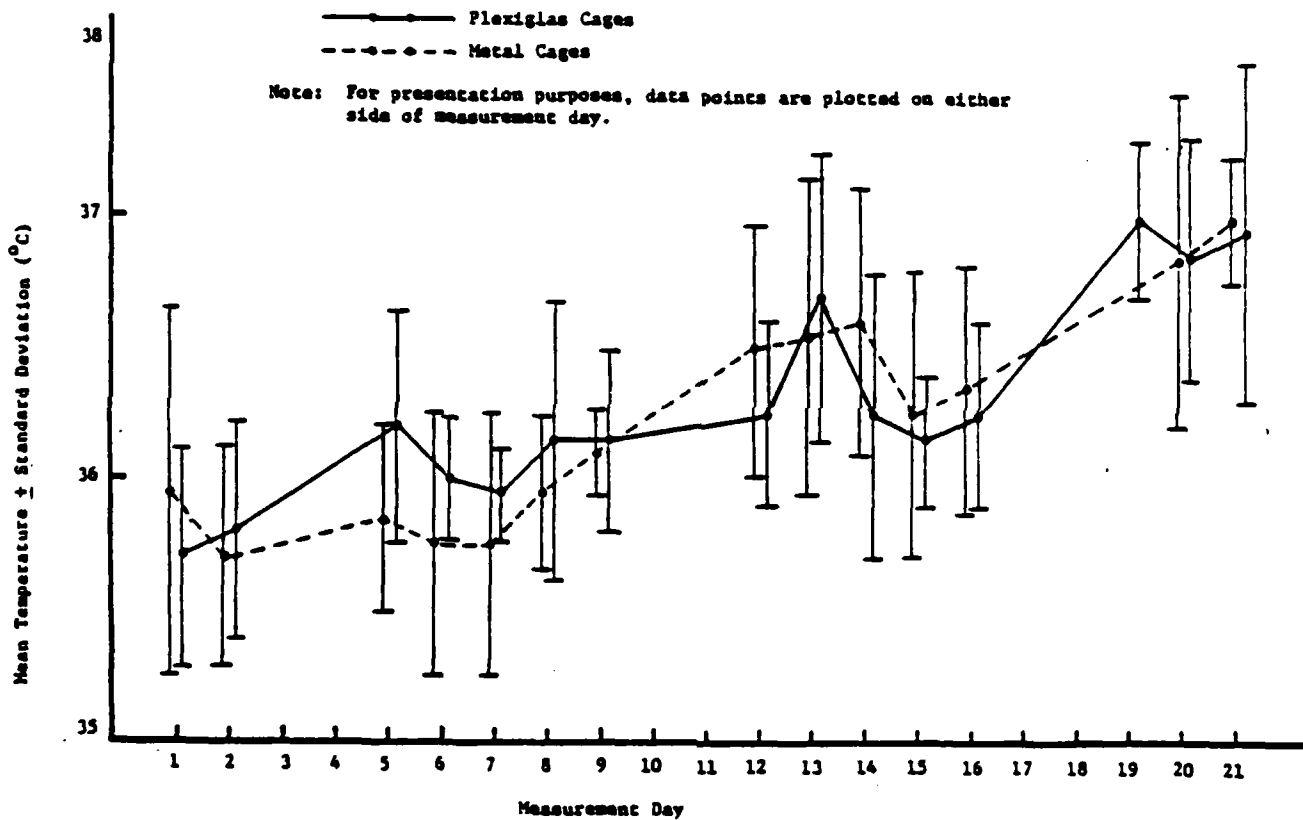


Figure 14. Comparison of body temperature of rats housed in Plexiglas cages to rats housed in standard metal cages.

During RFR exposure, the best position for the rats is parallel to the cage long dimension so coupling with the exposure field will be maximized. A five-level code was devised for scoring rat postural positions in the cages, and these positions were scored at random times during the day. The scoring defined whether the rats were parallel to the cage long dimension (Score 1), perpendicular to the cage long dimension (Score 5), or in some intermediate position (Scores 2, 3, or 4). Results of these 15-day observations were of concern because they clearly indicated that there was no preference for a position parallel to the cage long dimension. While the rats were young and small, there was a slight indication that a position perpendicular to the cage long dimension was preferred.

In an effort to urge the rats to position themselves parallel to the cage long dimension (and therefore parallel to electric field vector of the exposure field), modifications to the glass rod floors were made in two series of cages. Modifications to the first series of cages involved leaving the glass rods parallel to the cage long dimension, but positioning them such that rods in the cage center were slightly lower than those on either side. We thought that this uneven floor might urge the rats to position themselves along the level direction, i.e., parallel to the cage long dimension. For the other series of cages, all glass rods were level, but their orientation was changed such that they were perpendicular to the cage long dimension.

Using the previously described scoring system, postural preferences of the rats were observed over an 11-day period. Mean rat positions were calculated and compared with the results obtained during the initial observations. The comparison clearly indicated (mean rat positions were 3.41, 3.43, and 1.91, respectively, for the three floor arrangements) a desired postural position when the glass rods in the cage floors are perpendicular to the cage long dimension.

Subsequent to the evaluations of body weight, body temperature, and postural preference, minor design changes were made in the cage to facilitate provisions for watering and feeding. These changes involved moving the food hopper to the cage side next to the water bottle, and providing a Plexiglas frame to support a plastic water bottle in its desired position. The changes finalized the cage design with the final cage as shown in Figure 15.

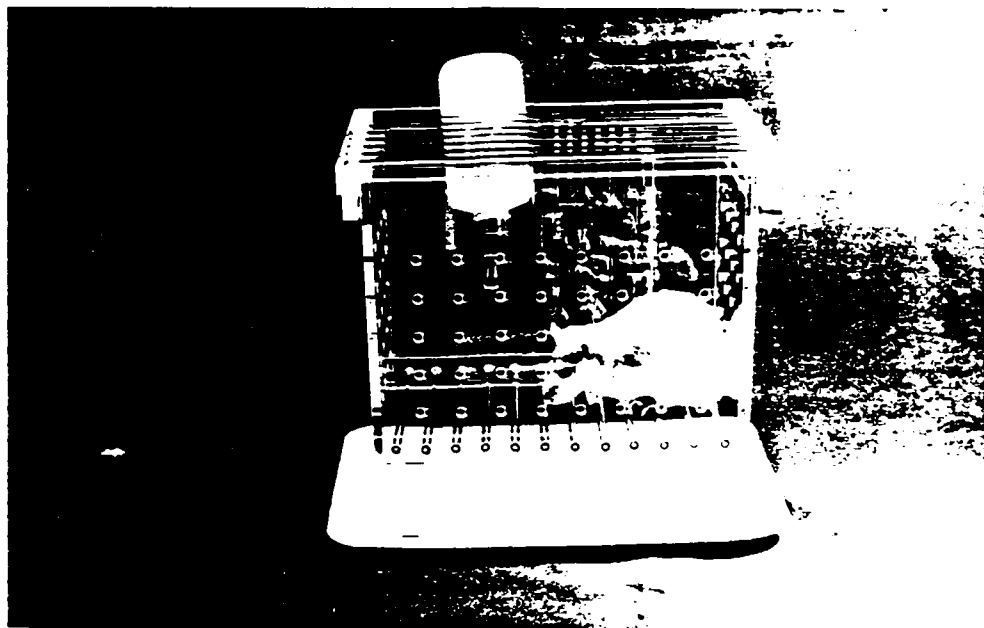


Figure 15. Final cage design showing changed water bottle and food hopper positions.

### Cage Separation Consideration

Once the cage design was established, concern was directed to defining the minimum separation distance that must be maintained between caged rats to assure an acceptable level of intercage scattering. As noted earlier, this separation distance was important because it dictated the exposure area that had to be illuminated during the study. We wanted to be able to define the extent to which the exposure field incident on one caged rat was influenced by the scattered exposure fields from all other caged rats. The definition of intercage scattering could be presented in such a way that scattering at the location of one caged rat was  $-X$  dB when the other caged rats are removed by  $Y$  centimeters, and  $-X \pm x$  dB when the other caged rats are removed  $Y \pm y$  centimeters. This definition would permit specifying intercage scattering in terms of  $-dB$  as a function of separation distance, and would therefore provide a very useful tool for determining minimum cage separation requirements for bioeffects studies.

Several approaches were considered for determining intercage scattering. In the first approach, experimental measurements using a near-field range were

considered. However, the available range was not equipped to accommodate frequencies as low as 450 MHz; therefore, frequency scaling would be necessary. This approach would require a corresponding scaling of dimensions and dielectric properties for both the cage and the rat. Uncertainties that could be introduced in the scaling, plus the time necessary to make the measurements, resulted in this approach being unattractive.

In the second approach, analytical solutions for intercage scattering were considered. The approach, however, required that a convenient geometry and dielectric property characterization be assumed for the cages and rats. Existing computer programs would then have to be modified to yield the exposure at one location due to the combined incident and scattered fields from other locations. Mathematically, the approach would be quite involved, and some verification of the predicted exposure field would be needed. In view of these considerations, we determined that this approach was beyond the scope of this study.

The use of a phase-center range was considered as the third approach. On this range, a probe antenna would be rotated in an arc centered at the caged rat, and the scattered fields would be measured. Difficulties with this approach emerged because limitations on the arc length traveled by the probe antenna were such that the forward scatter would not be satisfactorily measured, and a 450-MHz antenna with size, directivity, and weight as necessary for probing was not readily available.

Because of difficulties associated with the previously mentioned approaches, we decided that preliminary measurements should be made using the Georgia Tech compact range. The range gave both a readily available means for illuminating caged rats, and a reasonably satisfactory system for probing scattered fields. Six Plexiglas cages were constructed and used to house large male rats. These caged rats were positioned on a Styrofoam cage support structure in the exposure field. A tunable dipole antenna was adjusted to 450 MHz and mounted to a gear-driven mechanism that could travel either horizontally or vertically over a 213-cm (7 ft) path directly behind the caged rats. Using a 450 MHz exposure frequency and this probe arrangement, scattered field measurements were made using only the Styrofoam cage support structure, the cage support structure with empty Plexiglas cages positioned at various locations, and the cage support structure with caged rats positioned

at various locations. For each measurement, the dipole antenna was used to probe the existing fields. The resulting data, in the form of plots of total field amplitude and phase, yielded at least preliminary information about the nature and extent of field scattering. From these data, the following observations were made (note that, unless otherwise stated, the following data are relative to a condition in which one caged rat is positioned in the center of the Styrofoam cage support structure):

- The Plexiglas cages were essentially transparent at 450 MHz.
- When one caged rat was positioned on the cage support structure, an amplitude perturbation of about 1.5 dB occurred relative to the cage support structure alone.
- When a caged rat was added on either side of the center-positioned cage rat (33.02-cm (13 in.) separation distance), an amplitude perturbation of about 0.75 dB occurred.
- When caged rats were added to both sides of the center-positioned caged rat (33.02-cm (13 in.) separation distance), an amplitude perturbation of about 1.5 dB was noted.
- When a 25.4 cm (10 in.) separation distance was used and caged rats were added on both sides of the center-positioned caged rat, an amplitude perturbation of about 1.8 dB was noted.
- Scattered fields above and below the center-positioned caged rat were considerably less than side-to-side scattered fields.
- The addition of small pyramids of absorbing material (Emerson and Cumming Type NZ-1) did not reduce intercage scattering. In fact, the absorbing material appeared to introduce scattering of its own.

The preliminary nature of the previously mentioned observations is stressed, and it is noted that much more comprehensive efforts must be undertaken to precisely define intercage scattering in arrays of caged animals used during bioeffects studies. For the purpose of this study, the measured data indicated that, for caged rats placed 0 cm (0 in.), 1.0 cm (0.4 in.), and 20.3 cm (8 in.) from a center-positioned caged rat, the amplitude variation in the total field was about 2.4 dB, 1.8 dB, and 1.1 dB, respectively. We expected that larger separation distances would result in less field

perturbation; therefore, a 45.7-cm (18 in.) cage separation distance was selected for this study. Such a separation distance was assumed to provide negligible intercage scattering.



## VII. CAGE WASHER SYSTEM

After reviewing the technical specifications, cost, and size of cage washers from several manufacturers, the Southern Cross Model 900-A Dyna Jet Washer was purchased and installed in Room D of the RFR Facility (Fig. 16). The washer is of stainless-steel construction and provides fully automatic wash, rinse, and final rinse cycles for all types of animal cages and accessories. A tempered safety-glass viewing window is installed in the washer front. Loading of the washer is done from the left (soil) side, through a guillotine, pass-through door with a safety interlock feature that prevents washer operation until the door is closed. Exit is on the right (clean) side, through a pass-through door identical to the one on the entry side. Cage washing is provided by water jets from motor-driven, rotating, stainless-steel manifolds above and below the wash compartment. A 133-1 (35 gal) detergent tank below the wash compartment is used for the wash cycle. This tank contains a heavy-duty heating element with an external control, so wash water temperature can be varied from room temperature up to 190°F. The rinse cycle uses hot tap water from the building utility supply. For final rinse, a 102.6-1 (27 gal) tank with an automatic water-level controller is provided. External plumbing provides for the introduction of special final rinse fluids (distilled water, deionized water, etc.) and disinfectants.

Automatic reset timers control the wash and rinse time intervals as follows:

Wash Cycle:	0 to 10 min
Rinse Cycle:	0 to 10 min
Final Rinse Cycle:	0 to 1 min

These timers are wired such that any cycle can be omitted by adjusting the cycle timer to the "off" position. After the timers have been set to the desired cycle durations, the start button is pushed and the wash operation is automatically continued through all cycles.

To facilitate wash and rinse operations, special-purpose stainless-steel racks are provided for the Plexiglas cages and glass water bottles. Each of

these racks hold 4 cages and 49 bottles, respectively, in the wash compartment of the washer. The bottle rack provides a cover of stainless-steel mesh to prevent water jets in the washer bottom from forcing bottles out of the rack during wash and rinse cycles.

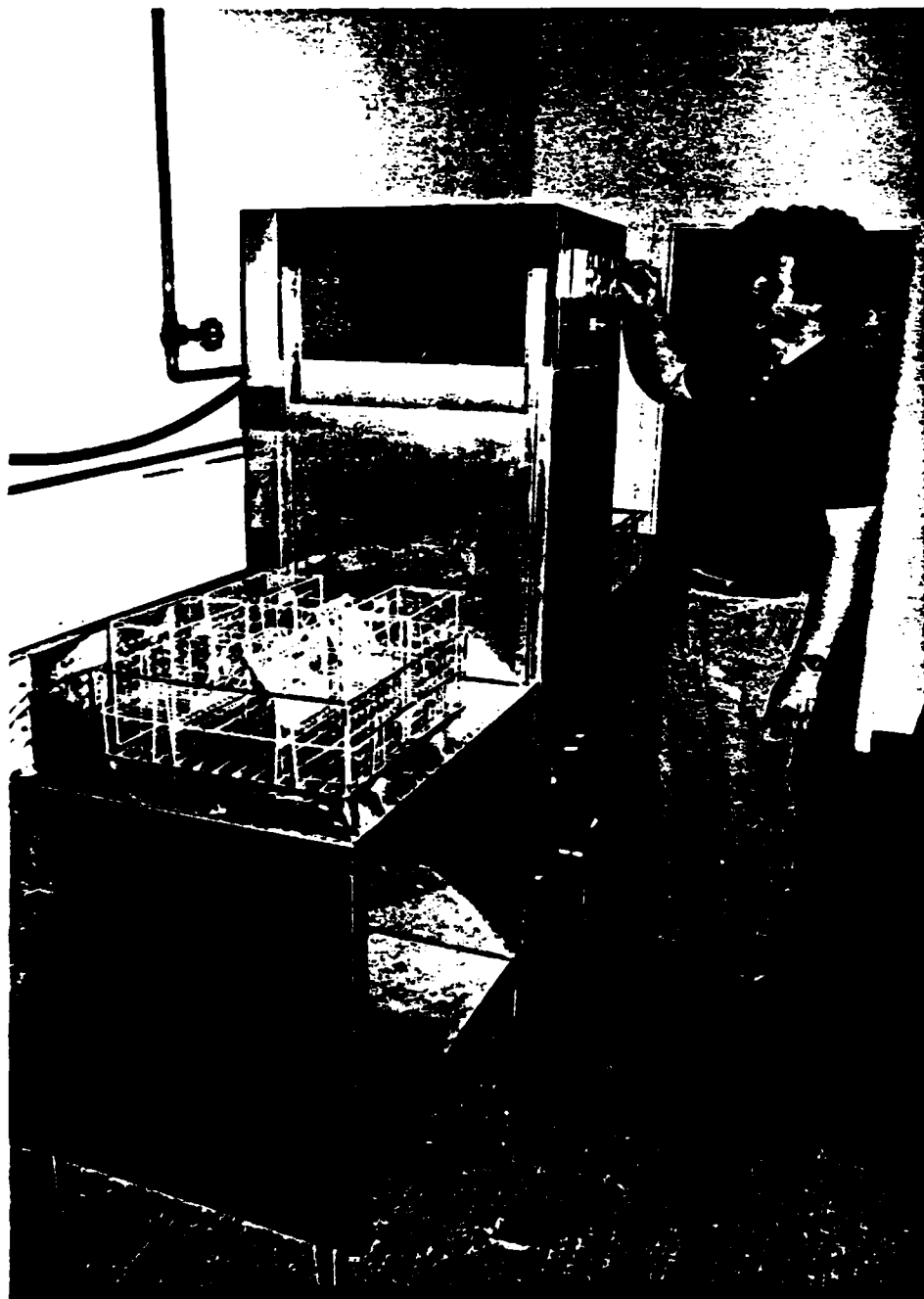


Figure 16. Cage Washer.

### VIII. DATA ACQUISITION SYSTEM

The long-term nature of this project dictated that a data acquisition and processing system would be desirable for storing experimental data and monitoring the RF facility. In particular, the system must:

- automate the data logging procedures,
- monitor the status of the exposure field,
- provide a home alert during non-work hours in case of system failure,
- perform basic statistical analysis of experimental data,
- interface with the Georgia Tech Cyber 70/74 mainframe for more extensive data processing, and
- be compatible with existing bioeffects systems established at the USAF School of Aerospace Medicine and the University of Washington.

With the foregoing system requirements in mind, a review of commercially available S-100 compatible computers was conducted. The review determined that both the Northstar Horizon and Cromemco System Two units were acceptable. Both units offered a system core consisting of S-100 motherboard; Z-80 8-bit processor chip as the Central Processing Unit (CPU); a 64 K Random Access Memory (RAM); two drives for 13.335-cm (5.25 in.) double-sided, dual-density disks; a controller; a cabinet; and necessary power supplies. Retail prices for the Northstar Horizon and Cromemco System Two units were \$4,330 and \$4,695, respectively. However, both systems were available at discounts of about \$750 from several different computer marketing centers. As capabilities of the two systems were compared in detail, we noted that either could be used for this program, but that the Cromemco System Two offered 390 kbytes/drive and a motherboard with 21 board slots. Comparable features of the Northstar Horizon system were 380 kbytes/drive and 12 board slots. On the basis of these differences in technical specifications, the Cromemco System Two unit was purchased.

To complete the system, peripherals and interfaces were needed for keyboard communication, printing, and I/O exchanges. The peripherals and interfaces chosen for the RF facility data acquisition system included:

- a Viewpoint CRT and keyboard (ADDS, Inc.) for terminal communications. A Cromemco Tuart board interfaces the terminal and the CPU,
- an Okidata 82A dot matrix printer for hard copy. Print speed is 120 characters/second with character spacings of 10 or 16.5 characters/inc. A Cromemco PRT board interfaces the printer and the CPU,
- A Cromemco D+7A I/O board to interface the CPU with a reference voltage indicating the status of the RF facility transmitter,
- A Pickles and Trout IEEE 488 Interface Board to allow communication between the CPU and the SARTORIUS balance system, or any other peripheral using 488 format, and
- A Sci-Tronics Real Time Clock Board to provide time and date information necessary for the system software requirements.

The RF facility data acquisition system uses the CROMEMCO CDOS 2.36 operating system. Application programs are written in the CROMEMCO 32 K Structured BASIC language (version 3.65).

## IX. ELECTRONIC BALANCE SYSTEM

An electronic balance capable of communicating with the data acquisition system was necessary for providing rat weight data. After reviewing technical capabilities of balances from several manufacturers, the Sartorius Model 1203 MP Balance with built-in microprocessor, variable integration time, and locked-in readout was purchased. The balance offered a weighing range and readability of 0 to 4000 g and 0.1 g, respectively. Besides the balance, a Sartorius Model 704201 Keyboard Programmer and Model 705306 Cable box were also purchased. The resulting electronic balance system was used to accurately weigh rats and automatically store the weight data in the data acquisition system. The keyboard programmer made it possible to program the balance for various different weighing procedures including net weight, mean weight, average weight, accumulated weight, and difference from a predetermined average weight. The weight displayed by the balance was actually the average of a programmed number of individual weighings performed over either a fast (0.5 s), normal (1 s), or slow (2 s) integration time. When the programmed number of weighings was completed, the average weight was locked in and displayed without fluctuation on a large, seven-segment digital readout. The taring capability of the balance was instantaneous and was done by touching the tare switch on the balance front. When the weight data displayed on the readout had achieved stability, a small "g" symbol appeared next to the weight value and indicated accurate data.

The following program was used to determine a rat's weight through the average of multiple weighings and associate this weight with the rat's identification number:

KEY	FUNCTION
g	Tare the balance Calls up stored regular weighing program
10	Key-in desired number of individual weighings (in this case, 10)
CS	Store the desired number of individual weighings

25 Key-in rat identification number (in this case, number 25)

# Transfer rat identification number to data output  
Place rat on balance pan

A Start program. The balance automatically weighs Rat # 25 ten times, displays the number of individual weighings, stores and adds up the individual weight values, calculates the mean weight, displays the mean weight, and transfers the mean weight value to the data output.

Place next rat on the balance pan

26 Key-in second rat's identification number (in this case, the number 26)

# Transfer rat identification number to data output

A Repeat weighing program for second rat

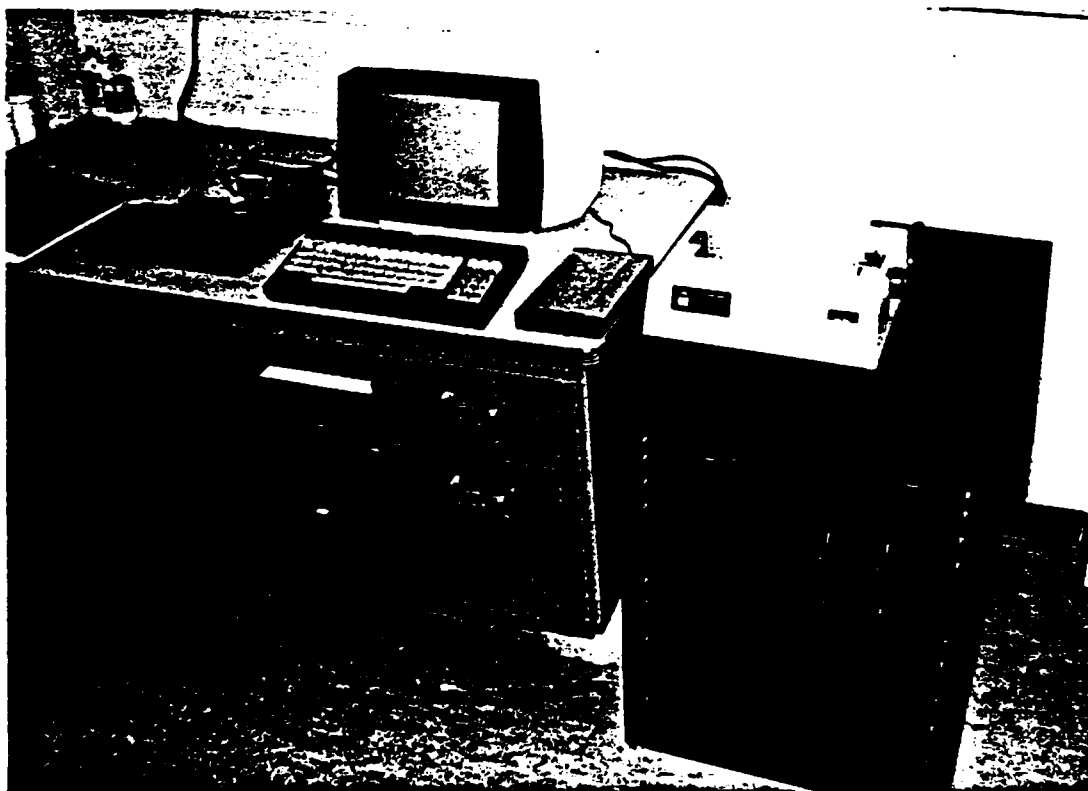


Figure 17. Electronic Balance/Data Acquisition System.

## X. OVERALL FACILITY DESCRIPTION

The overall facility for long-term exposure of large rodent populations to 435-MHz PW and CW environments consisted of (1) the four-tier assembly of circular, parallel-plate waveguides located in a radiation room, the walls of which were lined with microwave absorbing material, (2) an identical four-tier assembly of circular, parallel-plate waveguides located in a control room, the walls of which were also lined with microwave absorbing material, (3) a 435-MHz transmitter capable of either PW or CW operation that provided 4 outputs, each with 200 W average and 5.0 kW peak power, (4) 250 Plexiglas cages that individually housed rats during radiation exposure, (5) a room that housed the transmitter and its auxiliary equipment, (6) a room that housed devices needed for assay of biological endpoints, (7) a room that housed a cage washer/dryer, (8) a room that housed a computer-based data management system, (9) a room that stored food, cages, detergents, disinfectants, and other supplies, and (10) a buffer area that isolated the control and radiation rooms from other activity in the building. The cages, transmitter, and circular, parallel-plate waveguides have been described in previous sections of this report. In this section, the rooms for housing the facility are described.

The overall layout of the RFR facility is shown in Figure 18. The total facility occupied about 185.8 m<sup>2</sup> (2000 ft<sup>2</sup>) in Rooms 19 and 19A (basement level, northeast corner) of the Baker Building on the Georgia Tech main campus. The identification of each room in Figure 18 and its size are as follows:

<u>Room Purpose</u>	<u>Room Size</u>
Radiation room	7.01 x 7.01 m (23 x 23 ft)
Control room	7.01 x 7.01 m (23 x 23 ft)
Transmitter room	1.83 x 7.01 m (6 x 23 ft)
Buffer room	2.13 x 15.24 m (7 x 50 ft)
Computer room	3.04 x 3.04 m (10 x 10 ft)
Assay room	2.74 x 3.04 m (9 x 10 ft)
Clean-up room	2.74 x 3.04 m (9 x 10 ft)
Storage room	2.74 x 3.04 m (9 x 10 ft)

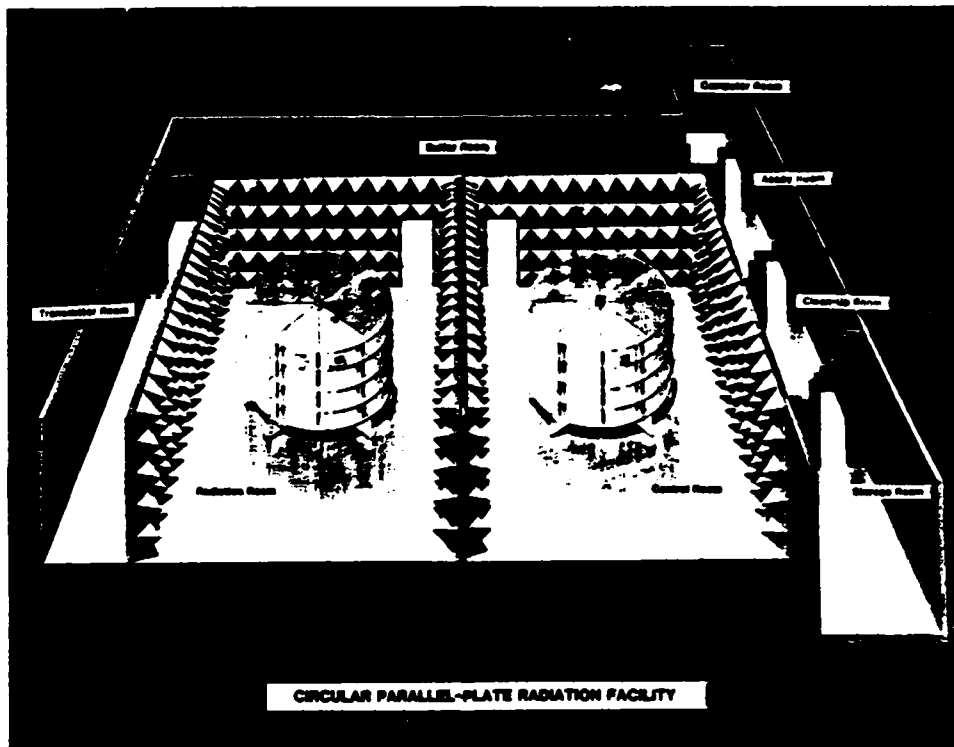


Figure 18. Overall layout of the RFR facility.



The microwave absorbing material lining the walls of the RFR and control rooms was purchased from Advanced Absorber, Inc., and has a height of 45.7 cm (18 in.). At 500 MHz, the specified reflectivity of this material was -30 dB. The material was mounted to the walls using Velcro hook and eye material. Strips of hook material were glued in appropriate locations to the sheetrock walls of the RFR and control rooms using contact cement. Similarly, strips of eye material were glued in appropriate locations to the absorbing material using contact cement. The approach made it possible to remove the absorbing material without tearing apart the individual blocks. All rooms making up the RFR facility were heated and/or cooled by an air-conditioning system isolated from the system used by the remainder of the Baker building. Since the facility is located in a corner area of the Baker building, two of its perimeter walls are outside walls; therefore, vents for the heating and cooling system were easily exhausted to outside air. This site was important for odor control and helped assure a disease-free rat colony. Lighting for the RFR and control rooms was powered by an automatic timer with a manual over-ride capability. The timers were used to cycle the lighting on a 6 AM-6 PM schedule. Temperature in these rooms was maintained between 70 and 74°C within a range of  $\pm 2^\circ\text{C}$ . Relative humidity was maintained at  $48 \pm 2\%$ . The control for this timer was at the entry to the rooms. Sheetrock used to form the perimeter walls for the RFR and control rooms was aluminum-backed, thereby providing a layer of foil shielding to reduce radiation leakage from the RFR Room. No extensive amount of shielding was necessary to control leakage radiation since these perimeter walls were lined with the microwave absorbing material. The common wall between the RFR and control rooms provided a double layer of foil shielding because aluminum-backed sheetrock was mounted to both sides of the studs for this wall. Shielding continuity between adjoining pieces of sheetrock was maintained by overlaying the aluminum foil from one piece of sheetrock to the next, then taping the seam with electrical-conductive aluminum tape. The ceiling for the RFR and control rooms consisted of 0.61 m x 0.61 m (2 ft x 2 ft) panels of acoustic tile suspended in a grid of T-supports. Each of these panels was covered with a layer of aluminum foil to reduce any radiation that might leak into office areas on the first floor level of the Baker building. Again, no extensive amount of shielding was considered necessary since the circular, parallel-plate waveguides directed

their radiation outward, not upward.

In the cage washer room, a 10-cm (4 in.) soil stack was provided as a drain for the cage washer. Also, 208 V, 3 phase power was available in this area for the cage washer. In the transmitter room, 208 V, 3 phase power was available for the transmitter. Dual receptacle outlets for 60 Hz, 115 V power were available in all rooms, including the RFR and control rooms, where the outlets were located behind the microwave absorbing materials.

## XI. REFERENCES

1. Tolar, J. C., R. L. Seaman, R. C. Johnson, and F. L. Cain, "Feasibility Study to Determine Design and Construction Criteria for a 420-to-450 MHz Chronic RFR Exposure Facility for Rats," Georgia Tech Final Report on Project A-2228, Subcontract No. SCEEE ARB/78-3, July 1979.
2. Guy, A. W., and C. K. Chou, "System for Quantitative Chronic Exposure of a Population of Rodents to UHF Fields," HEW Publication (FDA) 77-8011, Vol. II, pp. 389-410, October 20-23, 1975.
3. Guy, A. W., et al., "Specific Absorption Rates in Mice Exposed to 918 and 2450 MHz Circularly Polarized Guided EM Waves," Digest of Bioelectromagnetics Society Symposium, Seattle, WA, p. 426, June 18-22, 1979.
4. Oliva, S. A., and G. N. Catravas, "A Multiple-Animal Array for Equal Power Density Microwave Radiation," IEEE Trans. on MTT, pp. 433-436, May 1977.
5. "The Compact Range," Microwave Journal, Vol. 17, No. 10, pp. 30-33, October 1974.
6. Johnson, R. C., H. A. Ecker, and J. S. Hollis, "Determination of Far-Field Antenna Patterns from Near-Field Measurements," Proceedings of the IEEE, Vol. 61, No. 12 pp. 1668-1694, December 1973.
7. Johnson, R. C., H. A. Ecker, and J. S. Hollis, "Determination of Far-Field Antenna Patterns from Near-Field Measurements," Proceedings of the IEEE, Vol. 61, No. 12 pp. 1668-1694, December 1973.
8. Tolar, J. C., D. J. Freedman, and R. C. Johnson, "Prototype Circular, Parallel Plate Facility for Chronically Exposing Large Rodent Populations to 420-450 MHz Radiofrequency Radiation," Georgia Tech Final Report on Project A-2392, Subcontract No. SCEEE ARB/79-20, January 1980.
9. Kraus J. D., Antennas, McGraw-Hill Book Company, New York, 1950.
10. Blumlein, A., High Frequency Electrical Conductor or Radiator, U.S. Patent No. 2, 238, 770, April 15, 1941.
11. Jordan, E. C., and W. Miller, "Slotted Cylinder Antenna," Electronics, pp. 90-93, February 1947.
12. Sinclair, G. "The Patterns of a Slotted Cylinder Antenna," Proc. of IRE, pp. 1487-1492, December 1948.

13. Wait, J. R., "Radiation Characteristics of Axial Slots on a Conducting Cylinder," *Wireless Engineer*, pp. 316-323, December 1955.
14. Ramo, S., J. R. Whinnery, and T. Van Duzer, *Fields and Waves in Communication Electronics*, John Wiley, New York, 1965.
15. Bassen, H. I., et al., "A Miniature Broadband Electric Field Probe," *Ann NY Aca Sci*, 247:481-486 (1975).
16. "Responsibility for Care and Use of Animals," *NIH Guide for Grants and Contracts*, Vol. 7, No. 17, November 10, 1978, p. 1.
17. Melby, E. C., Jr., and N. H. Altman, *Handbook of Laboratory Animal Sciences*, CRC Press, Cleveland, OH, 1974, p. 451.
18. "Guide for the Care and Use of Laboratory Animals," *DHEW Publication No. (NIH) 78-23*, Revised 1978, pp. 34-35.
19. Toler, J. C., and C. L. Espy, "UHF Band Radio Frequency Radiation for Cardiac Pacemaker Studies," *Georgia Tech Final Report on Project No. A-1614, Air Force Contract No. F41609-74-C-0021*, June 1974, p. 15.
20. Catravas, G. N., "Styrofoam Cages for Rats Used in Microwave Research: Coating with Quinine," *Health Physics*, Pergamon Press, North Ireland, 1976, pp. 68-69.
21. Guy, A. W., and C. K. Chou, "System for Quantitative Chronic Exposure of a Population of Rodents to UHF Fields," *Biological Effects of Electromagnetic Waves*, Vol. II, *USDHEW*, December 1976.

END

2-87

DTIC